

Distribution Agreement

In presenting this thesis as a partial fulfillment of the requirements for a degree from Emory University, I hereby grant to Emory University and its agents the non-exclusive license to archive, make accessible, and display my thesis in whole or in part in all forms of media, now or hereafter known, including display on the World Wide Web. I understand that I may select some access restrictions as part of the online submission of this thesis. I retain all ownership rights to the copyright of the thesis. I also retain the right to use in future works (such as articles or books) all or part of this thesis.

Sabrina Lynn Stair

14 April 2011

A Comparison of Phosphodiesterase Type 4 (PDE4) Expression in the BLA in Control and
Chronically Stressed Rats

By

Sabrina Lynn Stair

Dr. Donald G. Rainnie, Ph.D.
Adviser

Program of Neuroscience and Behavioral Biology

Dr. Donald G. Rainnie, Ph.D.
Adviser

Dr. Michael Crutcher, Ph.D.
Committee Member

Dr. Kerry J. Ressler, MD, Ph.D.
Committee Member

Dr. E. Christopher Muly, MD, Ph.D.
Committee Member

14 April 2011

A Comparison of Phosphodiesterase Type 4 (PDE4) Expression in the BLA in Control and
Chronically Stressed Rats

By

Sabrina Lynn Stair

Dr. Donald G. Rainnie, Ph.D.

Adviser

An abstract of
a thesis submitted to the Faculty of Emory College of Arts and Sciences
of Emory University in partial fulfillment
of the requirements of the degree of
Bachelor of Sciences with Honors

Program of Neuroscience and Behavioral Biology

2011

Abstract

A Comparison of Phosphodiesterase Type 4 (PDE4) Expression in the BLA in Control and Chronically Stressed Rats

By Sabrina Lynn Stair

The basolateral nucleus of the amygdala (BLA) is the site of fear-learning, and is part of the neural circuitry disrupted in mood and affective disorders. Evidence suggests that phosphodiesterase 4 (PDE4) inhibitors, which enhance cAMP levels, could be potential treatments for affective disorders. In line with this, unpublished data from our laboratory reveals that PDE4 inhibition causes robust changes in the physiological properties of BLA principal neurons. Thus, aberrant PDE4 activity in BLA principal neurons may contribute to the development of affective disorders. There are approximately twenty-five known PDE4 isoforms, and little is presently known about the baseline expression of PDE4 mRNA and protein isoforms in the BLA. We performed RT-PCR, single cell RT-PCR, western blot analysis, and immunohistochemical analysis to elucidate the expression of PDE4 in the BLA. Our results indicate that of the PDE4A, PDE4B, and PDE4D mRNA transcripts we investigated, all PDE4 isoforms were expressed in the whole tissue BLA samples except PDE4D1 and PDE4D2. Moreover, we found that mRNA transcripts for most of these PDE4 isoforms were also expressed in BLA principal neurons, with the exception of PDE4B1, PDE4B2, and PDE4D8. Western blot and immunohistochemical analysis confirmed the presence of mature peptide for many of these same isoforms. Following exposure to a repeated, four day, unpredictable shock stress paradigm (USS), we found that PDE4A and PDE4D mRNA transcripts were down-regulated in whole tissue samples of the BLA. Importantly, PDE4D mRNA transcripts were also down-regulated in BLA principal neurons following USS. A semi-quantitative densitometric PCR analysis in whole tissue BLA samples revealed that PDE4A1, PDE4A5, PDE4A8, PDE4A10, PDEB3, PDE4B, PDE4D5, PDE4D7, PDE4D8, and PDE4D9 were significantly down-regulated following USS. These PDE4 isoforms may represent important targets for further investigation with quantitative PCR probes and isoforms specific antibodies. Overall, this project has taken the first steps in determining baseline expression of PDE4 isoforms in the BLA, an important task if PDE4 inhibitors are to be used as pharmacological treatments for mood disorders in the future.

A Comparison of Phosphodiesterase Type 4 (PDE4) Expression in the BLA in Control and
Chronically Stressed Rats

By

Sabrina Lynn Stair

Dr. Donald G. Rainnie, Ph.D.

Adviser

A thesis submitted to the Faculty of Emory College of Arts and Sciences
of Emory University in partial fulfillment
of the requirements of the degree of
Bachelor of Sciences with Honors

Program of Neuroscience and Behavioral Biology

2011

Acknowledgements

I would like to thank Dr. Donald Rainnie, Ph.D., Dr. Kerry Ressler, MD, Ph.D., Dr. E. Christopher Muly, MD, Ph.D., and Dr. Michael Crutcher, Ph.D. for serving as members of my honors thesis committee; their support, input, and advice have been invaluable throughout the duration of my project. I would also like to thank Dr. Rimi Hazra, Ph.D. and Dr. Joanna Dabrowska, Ph.D. for their continuous support and guidance throughout this process. They have aided me in all aspects of this process, from teaching me the research techniques to helping me to analyzing my data and format my figures. Their assistance has been indispensable, and greatly appreciated. I would also like to thank Dr. Jidong Guo, Ph.D., Dr. Chen-Chen Li, Ph.D., and Steven J. Ryan, B.S., Ph.D. candidate, for the contribution of both their data and their technical assistance throughout this process. Finally, I would like to extend a special thanks to Dr. Donald G. Rainnie, Ph.D., my thesis advisor. Without his continued guidance, support, occasional pushing, and funding, this project would not have been possible. The privilege of working in his laboratory has been one of the most rewarding educational experiences of my undergraduate career.

Table of Contents

Introduction.....	1
Methods.....	11
Results.....	18
Discussion.....	25
Figure 1.....	34
Figure 2.....	35
Figure 3.....	36
Table 1.....	37
Figure 4.....	38
Figure 5.....	39
Figure 6.....	40
Figure 7.....	41
Figure 8.....	42
Figure 9.....	43
Figure 10.....	44
Figure 11.....	45
Figure 12.....	46
Figure 13.....	47
Figure 14.....	48
Figure 15.....	49
References.....	50

Introduction

The basolateral nucleus of the amygdala: Anatomy and implications in mood disorder

The basolateral complex of the amygdala (BLC) is a pseudo-cortical structure situated in the temporal lobe that is part of the greater emotional circuitry consisting of the amygdala, hippocampus, perirhinal, and prefrontal cortices. The amygdala is a heterogenous structure composed of several different nuclei, including the BLC, which is composed of the lateral, basolateral, and accessory basal nuclei, each of which consist of roughly similar cell populations and microcircuitry (Rainnie & Ressler, 2008). Long known to be the site of fear conditioning (LeDoux, 2003), the BLC performs the evolutionarily important task of assigning emotional salience to stimuli. The BLC in particular seems important in mediating cross-modal associations, and appears to be a point of sensory convergence within the brain, being richly innervated by both the thalamus (Pitkänen, 1997) and the cerebral cortex (McDonald, 1998). Sensory inputs are relayed into the BLC through the lateral nucleus (LA) and the basolateral nucleus (BLA). From the LA, efferents are sent to the BLA and, more sparsely, to the central nucleus. The BLA also receives inputs from the entorhinal cortex, hippocampus, polymodal association areas, and the medial prefrontal cortex (Pitkänen, 1997; LeDoux, 2007).

Nearly 80% of the neuronal cell population within the BLA consists of glutamatergic pyramidal projection neurons, also called principal neurons. In addition, there are four main immunologically distinct interneuron populations: those that are immunoreactive for 1) parvalbumin (PARV; 40%), 2) somatostatin (SST; 20%), 3) cholecystokinin (CCK; 20%), and 4) calretinin and vasoactive intestinal peptide (CR/VIP; 20%). Recent electrophysiological evidence also suggests that the PARV interneurons may be further subdivided into at least two populations of electrophysiologically distinct neurons. Together the different interneuron

subpopulations help to tightly regulate the firing activity of principal neurons within the BLA. For example, activation of a subpopulation of interneurons results in feed-forward inhibition that can increase spike timing precision of principal neurons by limiting the window for temporal summation of excitatory synaptic inputs to 4 ms (reviewed in Rainnie & Ressler, 2009).

The central nucleus (CE), which receives inputs mainly from the BLA, is the major output nucleus for amygdala projections to the brainstem and hypothalamus (Pitkänen, 1997; LeDoux, 2007). It is the efferent projections of the central nucleus that mediate the physical responses of fear (reviewed in Davis et al, 1994). Additionally, the BLA also projects to the bed nucleus of the stria terminalis (BNST). The BNST has the many of the same outputs as the CE, but is believed to have more active role in modulating anxiety and vigilance; in contrast, the CE is involved in the expression of learned fear but not anxiety. Hence, lesions of the CE prevent the expression of learned fear, whereas lesions of the BNST prevent the enhanced expression of fear in the presence of natural stressors (Davis, 1997). Moreover, Walker and colleagues have postulated that while the CE is necessary for the rapid onset, short duration behaviors that occur in response to specific threats, the BNST is involved in the slower onset, longer lasting responses that accompany sustained threats (Walker et al., 2003). Significantly, the behavioral response to both short- and long-duration threats is blocked by inactivation of the BLA. Thus, activation of the BLA plays a major role in normal adaptive response to a wide variety of stressors. The afferent and efferent connections of BLC are summarized in Figure 1.

It is not surprising, therefore, that additional evidence suggests that abnormal regulation and hyperactivity of the fear circuitry within BLA may underlie psychiatric disorders such as major depressive disorder (MDD) and post-traumatic stress disorder (PTSD) (Rainnie & Ressler, 2009). For example, fMRI studies have revealed abnormally high neuronal activity within the

amygdala of depressed patients, in addition to increased amygdala size; only in the amygdala is this hyperactivity positively correlated with the severity of MDD (Drevets, 1999). Moreover, successful antidepressant regimens are accompanied by reduced amygdala activity as measured by fMRI, suggesting that abnormal amygdala activity may be a symptom of or a factor in the etiology of depression. Indeed, the absence of lowered amygdala activity when coupled with antidepressant treatment is a good predictor of patient relapse (Drevets, 1999).

Recently, a growing body of evidence has suggested that these changes in the BLA may be mediated via alterations in second messenger signaling cascades, specifically the cAMP/PKA cascade, reviewed below.

The cyclic AMP (cAMP)/Protein kinase A PKA second messenger cascade

There are two major classes of receptors in synaptic signaling: ionotropic receptors, whose activation causes the direct opening and closing of an ion channel, and metabotropic receptors, which couple to a second messenger cascade. Metabotropic receptors can be further subdivided into two classes, 1) those that couple to tyrosine kinase (trk) and 2) those that couple to G-proteins (GPCR). GPCRs have seven membrane spanning regions and associate with heterotrimeric G-proteins at their cytosolic domains. It is the identity of the G-protein α -subunit that determines the second messenger cascade to which the receptor is coupled. One such second messenger cascade is the cAMP/PKA pathway, which is activated by G_{α_s} and $G_{\alpha_{olf}}$, and inactivated by G_{α_i} . The cAMP/PKA pathway is illustrated in Figure 2. Briefly, neurotransmitter binding to the receptor causes the G_{α_s} subunit to exchange its bound GDP for a GTP. This exchange activates the G_{α} subunit, causing it to dissociate from the G_{β} and G_{γ} subunits. From there, G_{α} activates adenylate cyclase, which catalyzes the conversion of ATP into cAMP. cAMP,

in turn, activates protein kinase A (PKA) by binding to the PKA regulatory domain and freeing the catalytic domain, which then acts to phosphorylate multiple downstream target proteins.

Importantly, cellular cAMP levels are returned to baseline levels by the activity of a family of phosphodiesterase enzymes (PDE), which cleave cAMP into 5'-AMP (reviewed in Siegelbaum et al, 2000; Lodish, 2008).

PKA has many cellular targets, one of which is the cAMP-response element binding protein (CREB), a transcription factor that has been implicated in the consolidation of short-term memories into long term memories. PKA recruits mitogen-activated protein (MAP) kinase, and together they translocate to the nucleus, where PKA activates CREB-1 to bind the cAMP-response element (CRE), a promoter element, while MAP kinase removes the inhibition of gene transcription by CREB-2 (Kandel, 2001). CREB, in turn, regulates the transcription of many genes implicated in learning and memory, but in particular, brain-derived neurotrophic factor (BDNF), a neurotrophic factor that is implicated in neuronal growth and survival (Jessel & Sanes, 2000). As reviewed in Rattiner et al. (2005), BDNF has also been implicated in fear learning within the amygdala. BDNF mRNA levels, but not those of five other neurotrophins, were elevated in the BLA during the period following fear conditioning, peaking at two hours post-training. Moreover, the elevation was local to the BLA but not other amygdaloid nuclei. Hence, activation of the cAMP/PKA pathway can initiate a cascade of events that would greatly facilitate fear learning, and abnormal activation of this pathway may contribute to the etiology of affective disorders.

Significantly, Fadok and colleagues have shown that dopamine release within the BLA is necessary for fear learning to occur, and that this effect is dependent on activation of the dopamine type 1(D₁R) receptor family, which is highly expressed in the LA and BLA (Muly et

al., 2009). Moreover, dopamine deficient mice show major deficits in fear memory formation; however, selective restoration of dopamine transmission from the ventral tegmental area (VTA) to the BLA was sufficient to recover deficits in short-term, but not long term memory (Fadok et al., 2009). Moreover, fear memory formation was deficient in D₁R knockout mice but not D₂R knockout mice. Together, these data suggest that activation of the D₁R in the BLA is necessary for fear memory formation. Interestingly, the D₁R is coupled to G_s; thus, it appears that fear learning in the BLA is dopamine dependent and involves activation of the cAMP/PKA cascade. Consistent with this premise, unpublished observations from our laboratory show that D₁R antagonists block the induction of long-term potentiation (LTP) in the BLA, which is thought to represent the cellular substrate of memory formation, even in the presence of its downstream targets such as BDNF (Li and Rainnie, unpublished observation). Hence, any disruption of the cAMP/PKA signaling cascade coupled to the D₁R could have a significant impact on the induction of LTP and, as a result, fear memory formation.

The role of second messenger systems and phosphodiesterase type 4 in mood disorders and depression

Most current antidepressant treatments act by increasing the amount of monoamines, such as serotonin (5HT) or norepinephrine (NE) released and retained in the synapse. However, although the synaptic monoamine levels are rapidly increased by antidepressants, the therapeutic effects require weeks to months to appear (Andrade, 2010). It is now believed that increasing monoamine levels in the synapse itself does not attenuate depression; rather, it is the effect of these monoamines acting to regulate firing activity in multiple, connected, neural systems which has the primary effect in treating depression (Ressler & Nemeroff, 2000).

Over the past few decades, an overwhelming body of evidence has come to suggest that depression involves a deficit of synaptic plasticity in the mPFC and hippocampus and an increase in amygdala plasticity that is mediated via intracellular cascades (reviewed in Pittenger, 2008). Specifically, chronic stressors and acute glucocorticoid administration upregulated MAP kinase in the hippocampus, and acute and chronic stressors upregulated pCREB in the hippocampus but reduce BDNF mRNA. In turn, antidepressant treatments upregulated the cAMP/PKA/CREB pathway and increase the expression of BDNF in the hippocampus. Indeed, stress is a major precipitating factor in the etiology and expression of many affective disorders (reviewed in Pittenger et al., 2008), and it has been shown to alter neuroplasticity and enhance both amygdala-dependent fear learning (Rau, 2005) and decrease the threshold for LTP induction in the BLA (Li & Rainnie, unpublished observations). Taken together, this evidence suggests that stress and affective disorders are acting on the cellular pathways that underlie neuroplasticity and learning.

One source of connection between stress and depression is corticotrophin releasing factor (CRF), which is released in response to internal and external stressors. Patients suffering from affective disorders such as depression and PTSD exhibit heightened basal CRF levels and abnormal response to exogenously administered glucocorticoids. Moreover, increases in circulating glucocorticoids, whose release is stimulated by CRF, enhances fear learning, and this effect is blocked by BLA lesions (reviewed in Herbert et al., 2006). Specifically, Herbert et al. elucidated that activation of the CRF type 1 receptor (CRF₁), which has high expression in the BLA, but not CRF₂ receptor activation, is necessary for fear memory consolidation. Moreover, rats given CRF₁ antagonists also had reduced levels of phosphorylated cAMP (pcAMP) and pCREB, suggesting that CRF₁-dependent activation of the cAMP/PKA/CREB cascade was also necessary for stress-induced facilitation of fear memory consolidation (Hubbard et al, 2007).

Thus, CRF released in response to stress appears to enhance fear-learning by activating the same second messenger pathways as the D₁R.

Induction of LTP in the BLA is dependent not only on D₁ receptor activation (Fadok, 2009), but also on post-synaptic depolarization, calcium influx, and activation of the cAMP/PKA cascade (Huang et al, 1998). Specifically, bath application of the cAMP activator forskolin enhances LTP, while PKA inhibitors block LTP (Huang & Kandel, 1998). Taken together, these data suggest that increasing cAMP and PKA would lower the threshold for LTP induction. Indeed, unpublished results from our laboratory have revealed that elevating cytosolic cAMP levels with exogenous administration of rolipram, a selective PDE4 inhibitor, to BLA slice preparations acts to reduce the action potential firing threshold recorded in BLA principal neurons and facilitates the induction of LTP (see Figure 3a). These data suggest that modulation of PDE4 activity may be a potential site of action for factors that are involved in the etiology of affective disorders. Consistent with this premise, Zhang and colleagues have demonstrated that PDE4 inhibition by rolipram has antidepressant-like effects in behavioral models of depression (O'Donnell & Zhang, 2004).

In the central nervous system (CNS), the family of PDE4 enzymes is responsible for the conversion of cAMP into 5'-AMP, thereby lowering cellular cAMP back to basal levels following activation of the adenylate cyclase signaling cascade, and hence fine-tuning neuronal activity. Additionally, the PDE4 family of enzymes is almost exclusively responsible for the breakdown of cAMP generated by β -adrenoreceptor stimulation (O'Donnell & Zhang, 2004). There are four major PDE4 subfamilies, A-D, transcribed from four chromosomal locations of which all but C are differentially expressed in the CNS (for review see Houslay, 2007). There are approximately twenty-five known PDE4 splice variants spanning the four groups, and each

splice variant has a unique N-terminus region involved in localizing the enzyme to specific sites within the cell (Zhang, 2009). Some PDE4 enzymes also contain additional binding sites allowing macromolecular interactions with anchoring proteins such the A-kinase anchoring proteins (AKAPs) and the beta-arrestins (Houslay, 2007). It is believed that through specific localization, PDE4 is able to fine-tune intracellular levels of cAMP at specific loci within the cell.

Recent studies have shown that PDE4A and PDE4B subtype expression is increased in the frontal cortex with repeated antidepressant treatment (Takashi, 1999). Ye and colleagues have demonstrated that PDE4A1 and PDE4A5 expression is increased in the hippocampus and cerebral cortex with antidepressant treatment (Ye et al., 2000). On the otherhand, genetic deletion of PDE4D results in an antidepressant-like effect in constitutive PDE4D knock out (KO) mice (Zhang, 2002). Specifically, PDE4D KO mice but not controls or heterozygous littermates exhibited reduced immobility in the tail-suspension test and forced swim test. Additionally, immobility was further reduced by desipramine and fluoxetine in all groups, but rolipram only enhanced these effects in wildtype mice, suggesting that PDE4D is an essential mediator of the antidepressant effects of rolipram (Zhang et al., 2002). These seemingly conflicting data might result from differential expression of different PDE4 isoforms in different brain regions, or a differential response of PDE4 isoforms to environmental stressors. For example, Itoh et al. have demonstrated that, in rats, learned helplessness—a stress model of depression—causes an initial reduction of PDE4 activity in the frontal cortex (FC) followed by a delayed increase in activity in the FC and hippocampus. The authors postulated that a stress-induced hypofunction of the cAMP-dependent signal transduction system, mediated by increased PDE4 activity in the hippocampus and FC, may be related to chronic pathological states of depression (Itoh et al.,

2003). Consistent with this hypothesis, in the 1980s rolipram was shown to have considerable promise as a novel antidepressant because of its rapid therapeutic onset; however, emetic side effects have precluded its clinical use (Zhang, 2009). Theoretically, because of the diversity of PDE4 subtypes it may be possible to separate the emetic side effects of rolipram from its clinical efficacy; however, little is presently known about the differential expression of PDE4 in the emetic brain centers compared to that in emotional circuitry of depressed and normal individuals.

As mentioned previously LTP is thought to represent the cellular substrate for fear learning (Kandel, 2000). It is noteworthy, therefore, that inescapable stress has been shown to prevent the induction of LTP in the efferent pathway from the BLA to the medial prefrontal cortex (Maroun & Richter-Levin, 2003), whereas the same stressor blocks the induction of long-term depression (LTD) in the reciprocal pathway from the mPFC to the BLA and decreases the threshold for LTP induction (Maroun, 2006). Altogether, these findings suggest that stressors enhance fear memory in the BLA while reducing the regulatory inputs of other cortical areas.

Specific Aims of this Project

As mentioned above, exogenous administration of rolipram reduces the action potential firing threshold recorded in BLA principal neurons and facilitates the induction of LTP (Figure 3a), suggesting that inhibition of PDE4 could contribute to the hyperactivity of the BLA that has been linked to depression. Consequently, it would be of particular interest to know which PDE4 isoforms are expressed in principal neurons of the BLA, and whether or not these isoforms may be modulated by stress. However, little is known about baseline PDE4 isoform expression in the BLA, or their response to stress.

To fill this knowledge gap, we have used a multidisciplinary approach employing electrophysiological, molecular, and immunohistochemical techniques to elucidate the expression of select PDE4 subtypes within principal neurons of the BLA, from both control and stressed rats. Additionally, we will look at whole tissue expression of PDE4 subtypes in the BLA. Given that the amygdala demonstrates a hyperactive profile in both depressed patients and has been implicated in the stressed amygdala, and given that PDE4 is the main regulator of cytosolic cAMP levels, we predict that PDE4 would be downregulated in the BLA following the chronic unpredictable shock stress paradigm.

Methods

Animals

Sprague-Dawley rats were group housed, kept on an artificial 12 : 12 h light cycle, kept at 22°C, and given access to water and food ad libitum. All experimental protocols conform to the National Institutes of Health Guidelines for the Care and Use of Laboratory Animals, and were approved by the Institutional Animal Care and Use Committee of Emory University.

Whole Tissue RNA isolation and cDNA preparation

RNA isolation and cDNA preparation were performed as previously described by Hazra et al. (Hazra et al., 2011) and performed under the supervision of Dr. Rimi Hazra, Ph.D. Under isoflurane anesthesia, rats were decapitated and the brain quickly dissected out and placed into cold (4°C) 95-5% oxygen/carbon dioxide oxygenated “cutting solution” of the following composition (in mM): NaCl (130), NaHCO₃ (30), KCl (3.50), KH₂PO₄ (1.10), MgCl₂ (6.0), CaCl₂ (1.0), glucose (10). Coronal brain sections (500 µm) were sliced on a Leica VTS-1000 vibratome and tissue containing the BLA and BNST was excised by microdissection. RNA was then isolated and cDNA prepared from BLA and BNST tissue of eight (n=4 control, n=4 USS) rats according to the following protocol. Briefly, 100mg of tissue was homogenized in 1000 µL Trizol Reagent. The isolated RNA was then reverse transcribed using a cocktail containing 5 µl of 10XRT buffer, 10mM dNTP mix, 10X random hexanucleotide and Multiscribe RT 5U/ul and RNAase free water. The mixture was incubated in a thermal cycler at 25°C for 10 min and then at 37°C for 120 min. The resulting cDNA samples were stored at -20°C.

Single Cell cDNA isolation

Slices were obtained for electrophysiological recording purposes using the same procedure as outlined above except that prior to sectioning the brains were placed in a “cutting solution” with the following composition (in mM): NaCl (130), NaHCO₃ (30), KCl (3.50), KH₂PO₄ (1.10), MgCl₂ (6.0), CaCl₂ (1.0), glucose (10), supplemented with kynurenic acid (2.0). Slices containing the BLA were cut at a thickness of 350 μM using a Leica VTS-1000 vibratome (Leica Microsystems Inc., Bannockburn, IL, USA) (described in Guo & Rainnie, 2010). Slices were kept in oxygenated “cutting solution” at room temperature for 1 h before transferring to regular artificial cerebrospinal fluid (ACSF) containing (in mM): NaCl (130), NaHCO₃ (30), KCl (3.50), KH₂PO₄ (1.10), MgCl₂ (1.30), CaCl₂ (2.50), and glucose (10). Slices were kept in the regular ACSF for at least 30 min before recording. This protocol was previously published by our laboratory in (Guo & Rainnie, 2010).

After establishing that cells had the physiological properties consistent with their being BLA principal neurons, the cytosolic contents of the cells were aspirated into the recording electrode and then expelled into a microcentrifuge tube containing 5 μl of a reverse transcription (RT) cocktail by applying positive pressure. The single cell RT-PCR procedure then followed the protocol outlined above for whole tissue cDNA isolation. The resulting single cell cDNA was then amplified in triplicate and screened using the 18s rRNA as a control housekeeping gene to normalize for loading differences. Using cDNA obtained from ten cells, we performed qualitative PCR using standard procedures, outlined below, for each of the PDE4 isoforms, then visualized the resulting DNA by ethidium bromide staining following separation by electrophoresis in a 1-2% agarose gel. This protocol was previously published by our lab (Hazra

et al., 2011) and performed under the supervision of Dr. Rimi Hazra, Ph.D. Electrophysiological recording and single cell mRNA aspiration was performed by Dr. Jidong Guo, Ph.D.

Qualitative RT-PCR

RNA isolated from whole tissue and reverse transcribed according to the above protocols was added to a cocktail consisting was 10X PCR buffer, 3mM MgCl₂, 10mM dNTPs, 2.5U of Taq DNA polymerase, and 100nM of PCR primers. PCR primers used for each of the PDE4 isoforms were developed from GenBank sequences with commercially available Oligo software (IDT Tools, Coralville, IA, USA). The housekeeping gene 18S rRNA was used in all experiments as a positive control. PCR was performed on a PTC-200 Peltier thermal cycler (BioRad, Hercules, CA) using the following program: 94°C for 40 sec, 56°C for 40 sec and 72°C for 1 min for 40 cycles. PCR products were visualized by staining with ethidium bromide and separated by electrophoresis in a 1% agarose gel. Refer to Table 1 for the primer sequences and length of resulting product. As before, this protocol was developed by Dr. Rimi Hazra, Ph.D. (Hazra et al., 2011) and performed under her supervision.

Real Time Quantitative PCR (qPCR)

qPCR was performed on an Applied Biosystems 7500 Fast-Real Time PCR system (Applied Biosystems, Foster City, CA) according to the protocol published in (Hazra & Rainnie, 2011). RNA was prepared as outlined above for either whole tissue or single cell cDNA. Tests were carried out with TaqMan gene expression reagents purchased from Applied Biosystems (Foster City, CA) using pan primers for the PDE4A, PDE4B, and PDE4D subfamilies, which were acquired from Applied Biosystems (Carlsbad, California). All expression levels are

normalized to the 18s rRNA housekeeping gene, and data were analyzed using an unpaired student's T-test.

Western Blot

To determine the baseline PDE4 protein expression in the BLA, tissue samples were dissected as outlined for RNA isolation, and then homogenized in buffer containing protease inhibitors, 5mM HEPES, and 0.32 M sucrose (pH=7.4) according to the protocol described in (Dabrowska & Rainnie, 2010). Protein concentration was determined using a bicinchoninic acid assay, and 25 mgs of protein per sample was loaded onto polyacrylamide-SDS mini-gels, separated electrophoretically, blotted onto nitrocellulose membranes, and blocked for 1h in buffer containing 2% nonfat dry milk, 0.1% Tween 20, 0.05 M NaCl, and 1M HEPES (pH 7.4). The membranes were incubated overnight at 4°C with the following rabbit polyclonal primary antibodies: anti-pan PDE4A, 1:1000; anti-pan PDE4B, 1:500, anti-PDE4B3, 1:1000, and anti-pan PDE4D, 1:500 (FabGennixInc, Frisco, TX). Membranes were then incubated with an HRP-labeled specific secondary antibody (1:2000) for 1 hr at room temperature and then samples were detected using chemiluminescence and visualized with an Alpha InnotechFluorochem imaging system. As a loading control, membranes were probed again with a mouse monoclonal primary antibody raised against glyceraldehyde-3-phosphate dehydrogenase (GAPDH). Western blot analysis was performed under the supervision of Dr. Rimi Hazra, Ph.D. or Dr. Joanna Dabrowska, Ph.D.

Immunohistochemistry

Dual immunofluorescence was performed according to the protocol previously published by Dabrowska and Rainnie (2010). Dual-immunofluorescence experiments were performed on 4% paraformaldehyde-fixed rat brain sections derived from eight adult (45–60-days old) rats. Coronal brain sections (50 μ m) were cut on a Leica CM 3050S cryostat and stored at $-20\text{ }^{\circ}\text{C}$ in a cryoprotective medium consisting of 25% glycerol and 30% ethylene glycol in 0.05 M phosphate buffer until needed.

To examine the relative expression of the PDE4 in the BLA, we performed immunofluorescence or dual immunofluorescence on free-floating serial sections of the rat BLA. Representative sections were rinsed 3 \times for 10 min in PBS, permeabilized with 0.5% Triton-X 100 in PBS, and incubated for 48 h at $4\text{ }^{\circ}\text{C}$ with the primary antibody(1:500, polyclonal, rabbit) in 0.5% Triton-X/PBS solution with either mouse polyclonal antibody raised against calcium/calmodulin-dependent protein kinase α II (CaMKII α) (1:250) or parvalbumin (PARV) (1:250). Sections were then rinsed 3 \times for 10 min in PBS and incubated at room temperature for 2 h with Alexa-Fluor 488 goat anti-mouse IgG and Alexa-Fluor 568 goat anti-rabbit IgG (1:500, Molecular Probes, Invitrogen, Carlsbad, CA, USA). Following incubation, sections were rinsed 3 \times for 10 min in PBS, and 1 \times in phosphate buffer (PB), mounted on gelatin-coated glass slides and coverslipped using Vectashield mounting medium (Vector Laboratories, Inc., Burlingame, CA, USA). Dual-immunofluorescence analysis was accomplished by focusing on neurons throughout the thickness of the section and by maintaining the same focal plan switching between filter sets to ascertain if the cell shows dual immunofluorescence. Confocal spinning disk laser microscopy was used to obtain high-resolution photomicrographs (63 \times magnification)

using an Orca R2 cooled CCD camera (Hamamatsu, Bridgewater, NJ, USA) mounted on a Leica DM5500B microscope (Leica Microsystems, Bannockburn, IL, USA)

Unpredictable Shock Stress

Before administering the unpredictable shockstress, rats, thirty-five days of age, were first matched for their basal anxiety level using a standard acoustic startle paradigm (see Fox et al., 2008). Animals were then divided into two cohorts of 4 animals. Control animals received the same handling procedures as the unpredictable shock stress (USS) group without being shocked. Once the baseline startle response was measured (see below), on day 1 the USS rats received two eight minute periods of eight randomly applied footshocks (0.5s, 0.5 mA) separated by an eight minute period of no shock. The paradigm was repeated on each of the following three days for a total of four consecutive days shock stress. Each rat was shocked at approximately the same time every day to control for diurnal hormone variations. Rats in the control group are placed into the shock chamber for the duration of the paradigm, but do not receive a shock. On the tenth day, the post-test startle response is measured and the rats are sacrificed for tissue analysis (see Figure 4).

Baseline Startle Measurement

Here, the rats were placed in an acoustic startle chamber and allowed to acclimatize for 5 minutes. Startle responses were evoked by 50 ms 100, 105, and 110 dB white-noise bursts presented in pseudorandom order by a Macintosh G3 computer (Apple Computers, Inc.) sound file, amplified by a Tandy amplifier (model MPA-200; RadioShack), and delivered through speakers located in the front of each cage. Startle response amplitudes were quantified using an

accelerometer (model U321AO2; PCB Piezotronics) affixed to the bottom of each cage. Cage movement produced by the rats' startle response results in displacement of the accelerometer, which in turn produces a voltage output proportional to the velocity of cage movement. This output is amplified and digitized by an InstruNET device (model100B; GW Instruments) interfaced to a Macintosh G3 computer. Startle amplitude is defined as the maximal peak-to-peak voltage that occurred during the first 200 ms after onset of the startle-eliciting white-noise burst. The presentation and sequencing of all stimuli was under the control of the Macintosh G3 computer using custom-designed software (The Experimenter; Glassbeads Inc.)

Statistics

Behavior data pre-tests were compared using Students unpaired t-test, two-tailed, between the control and USS group prior to group assignment to ensure that baseline startle was not significantly different. Following post-test, the pre- and post-startle were compared between groups using the Student's paired t-test, one-tailed, to determine whether startle was significantly enhanced following USS.

All PCR data were normalized to 18s rRNA subunit mRNA expression, which served as a control for total mRNA within a sample. Cells expressing abnormal levels of 18s were excluded from data analysis. Following normalization, means were compared using an unpaired one-tailed student's T-test. For densitometric analysis, the raw data was further processed to cancel out any background noise and to control for the total amount of mRNA loaded into the ethidium bromide infused agarose gel before normalization.

Results

Baseline PDE4 Profile

Because there has been very little previous research on the basal expression of PDE4 isoforms within the BLA, and the available work is often contradictory (Perez-Torez et al., 2000; Miro et al., 2002; McPhee et al., 2001; Bolger et al., 2004) and not focused on the BLA, we used whole-tissue RT-PCR, single cell RT-PCR, western blot, and immunohistochemical analysis to examine the relative expression of PCR transcripts and peptide in BLA samples from control animals.

RT-PCR

We designed primers for sixteen of the PDE4 isoforms. Of the different isoforms we investigated, the RT-PCR results revealed that the mRNA for multiple isoforms of PDE4 are expressed in the BLA; namely PDE4A1, PDE4A5, PDE4A8, PDE4A10, PDE4B1, PDE4B2, PDE4B3, PDE4B4, PDE4D3, PDE4D4, PDE4D5, PDE4D7, PDE4D8 and PDE4D9, while PDE4D1 and PDE4D2 are not. These data are summarized in Figure 5.

Single Cell RT-PCR (scRT-PCR)

Given that we have shown enhanced LTP in BLA principal neurons following unpredictable shock stress (Fig 3b), and that this was mimicked by intracellular infusion of the PDE4 inhibitor rolipram into principal neurons (Fig 2a), we were particularly interested in elucidating the PDE4 expression profile of this cell type. Because the BLA is diverse in its cellular population, we performed scRT-PCR on neurons that had been classified as BLA principal neurons via electrophysiological profile (n=10). An example of a BLA principal

neuron, along with its electrophysiological profile, is given in Figure 6. Our scRT-PCR revealed the presence of PDE4A1, PDE4A5, PDE4A8, PDE4A10, PDE4B3, PDE4B4, PDE4D3, PDE4D4, PDE4D5, PDE4D7, and PDE4D9 but not PDE4B1, PDE4B2, PDE4D1, PDE4D2, or PDE4D8 in BLA principal neurons. In particular, PDE4B1, PDE4B2, and PDE4D8 were present in whole tissue but not principal neurons, suggesting their expression is restricted to other cell populations in the BLA.

Western Blot Analysis

Although our RT-PCR studies suggested that multiple isoforms of PDE4 could be expressed in principal neurons, mRNA expression does not always predict mature protein expression. Consequently, to confirm the presence of mature PDE4 peptide in the BLA, we performed western blot assays to examine PDE4 protein expression in the BLA from control animals. For these studies, we used antibodies against pan PDE4A, PDE4A5, pan PDE4B, PDE4B3, and pan PDE4D. Probing with the pan PDE4A antibody revealed bands for PDE4A1 (66 kDa), PDE4A? (76 kDa), and either PDE4A5, PDE4A8, or PDE4A10, indistinguishable due to the similarities in the predicted size (109, 106 and 108 kDa, respectively). Expression of PDE4A5 was independently confirmed using the specific PDE4A5 antibody, which revealed robust protein expression. The PDE4B pan antibody revealed bands for PDE4B2 (78 kDa) and PDE4B4 (66 kDa), while the PDE4B3 antibody revealed robust expression of PDE4B3 (100 kDa). The pan PDE4D antibody revealed the presence of PDE4D1 and/or PDE4D2 (both 68 kDa), PDE4D3 (95 kDa), and PDE4D5 (105 kDa). These results are summarized in Figure 7.

Immunohistochemistry

Having established that the mature peptide of multiple PDE4 isoforms was expressed in the BLA using western blot analysis, we next performed immunohistochemical staining against PDE4A, PDE4A5, PDE4B, PDE4B3, PDE4B4, and PDE4D to reaffirm the presence of peptide in whole tissue BLA (Figure 8). Additionally, we performed a dual-immunohistochemical study to determine the relative expression of some of these peptides in principal neurons and a subpopulation of parvalbumin (PARV) containing interneurons. This technique afforded us the chance to explore the distribution of PDE4 isoforms across the BLA cell populations. Here, we visualized principal neurons using an antibody directed against calmodulin-dependent protein kinase II alpha (CaMKII α), and a subpopulation of interneurons using an antibody directed against the calcium binding protein PARV. Neurons were dual labeled with antibodies directed against PDE4A5 or PDE4B3. The sample amount of PDE4B4 antibody donated to us was insufficient to perform co-localization experiments; thus, we were unable to perform dual-immunofluorescence experiments. Nevertheless, immunohistochemistry revealed that PDE4B4 was expressed in whole tissue BLA, although we cannot narrow it down to any specific neuronal population.

As demonstrated in Figure 8, our immunofluorescence experiments revealed that PDE4A is expressed richly throughout the BLA, and label was observed in both the soma and neuropil. Pan PDE4B was also expressed throughout the BLA, although it appeared to be localized primarily in the soma and less in the neuropil. In contrast, selective labeling with the PDE4B4 antibody appeared most prominently in the neuropil. Unfortunately, we did not have enough of the antibody to confirm this observation with dual-immunofluorescence. Finally, the PDE4D

signal was mostly confined to the soma, where it appeared to label an undetermined intracellular structure.

To determine the expression of PDE4 isoforms within specific cell populations, we co-stained with PARV and CamKII α to elucidate expression in parvalbumin immunoreactive interneurons and principal neurons, respectively. As summarized in Figures 9 and 10, PDE4A5 and PDE4B3 are expressed in both populations of cells.

Behavioral and cellular response to unpredictable shock stress (USS)

Behavioral response to repeated USS

Prior to receiving the unpredictable shock stress (USS), 8 rats were tested for their baseline acoustic startle in response to three different intensities of white noise, 100, 105 and 110 dB. The graded intensity measure allowed us to examine any alteration in the sensitivity to the startle stimulus resulting from the stress manipulation. Rats were then matched according to their baseline startle response and assigned to either the control or stress group such that, at day 0, there was no significant difference in the mean startle amplitude (mean pre-test amplitude control group = 0.55 vs stress group = 0.59, $p > .05$). As illustrated in Figure 11, following unpredictable shock stress, rats had a significantly increased startle response on day 10 as compared to baseline ($p < .05$) that was not detected in age matched litter mate controls (mean post-test amplitude control group = 0.54 vs stress group = 0.73). Moreover, the startle response was enhanced at all three dB levels tested.

Effects of Stress on whole tissue expression of PDE4 isoforms in the BLA

qPCR

Given the extensive body of evidence which suggests PDE4 is altered in response to both antidepressant treatment and stressful stimuli, and given that our unpublished data reveals that PDE4 inhibition and unpredictable shock stress both reduce the stimulus threshold necessary to induce LTP (Figure 3a&b), we next investigated whether the repeated USS paradigm would alter PDE4 gene expression in the BLA. To determine whether PDE4 mRNA expression is altered following USS, we performed qPCR on whole tissue BLA samples from control and USS rats. Additional samples were obtained from the hippocampus and BNST to evaluate region specific versus global changes in PDE4 expression. Following qPCR, data was analyzed and the outliers, as determined by aberrant 18s expression, were removed. For BLA the final sample sizes were n=4 for NS, n=4 for SS; hippocampus, n=3 for NS and n=4 for SS; BNST, n=4 for NS, n=3 for SS. Samples from each animal were run in triplicate to minimize sampling errors. As seen in Figure 12, repeated USS caused a significant down-regulation in PDE4A and PDE4D expression in the BLA ($p<.05$) while PDE4B mRNA also showed a trend towards up-regulation that was not significant. In contrast, expression of PDE4A and PDE4D was not significantly altered in the BNST following USS, but PDE4B showed a significant up-regulation ($p<.05$). We found no significant alteration in PDE4 gene expression in the hippocampus.

Qualitative PCR and densitometric analysis

At the time of this study, qPCR probes were not available for the specific PDE4 isoforms. So, to investigate the effects of USS on specific PDE4 isoform expressions, we performed

quantitative PCR on tissue from control (n=4) and USS (n=4) animals and then performed a densitometric analysis to evaluate any stress-induced changes. Our analysis revealed that PDE4A1, PDE4A5, PDE4A8, PDE4A10, PDE4B1, PDE4B2, PDE4B3, PDE4D3, PDE4D7, PDE4D8, and PDE4D9 were all significantly down-regulated ($p < .05$) following USS compared to controls. Furthermore, PDE4D5 mRNA showed a trend toward significant down-regulation ($p = .059$). PDE4B4 and PDE4D4 expression was not significantly altered, and PDE4D1 and PDE4D2 were not detected in either tissue, and therefore could not be analyzed. The results are summarized in Figure 13.

Single cell expression of PDE4 isoforms is altered by unpredictable shock stress.

Having established that USS caused a significant alteration in whole tissue mRNA expression we next examined whether USS also altered the expression of PDE4 mRNA specifically in BLA principal neurons. To this end, we reverse transcribed cDNA from principal neurons following electrophysiological recording and performed both qPCR using the available pan probes and qualitative single cell PCR (scRT-PCR) accompanied with densitometric analysis (control n=5, USS n=5).

qPCR

Our quantitative PCR revealed that PDE4D mRNA was significantly down-regulated in principal neurons following USS ($p < .001$). In addition, consistent with our whole tissue results, PDE4A mRNA expression was seen to trend towards a significant down-regulation ($p = .056$), whereas PDE4B mRNA expression was unaffected by USS. These data are summarized in Figure 14.

Qualitative PCR and densitometric analysis

Although we had shown that USS altered the expression of pan PDE4 isoforms in whole tissue samples of the BLA, the source of the deficit was not known. Moreover, large changes in individual PDE4 isoform expression could be masked in measurements of net mRNA changes using the pan PDE4 qPCR. Hence, we used qualitative PCR in conjunction with densitometric analysis to evaluate the expression of individual PDE4 isoform expression in BLA principal neurons. Our qualitative PCR was surprisingly consistent with the results found in whole tissue scRT-PCR. Hence, analysis of principal neuron mRNA revealed the presence of transcripts for the PDE4A1, PDE4A5, PDE4A8, PDE4A10, PDE4B3, PDE4B4, PDE4D3, PDE4D4, PDE4D5, PDE4D7, and PDE4D9 isoforms, but not the PDE4B1, PDE4B2, PDE4D1, PDE4D2, or PDE4D8 isoforms. Moreover, our densitometric analysis revealed that, of the all isoforms expressed in BLA principal neurons, PDE4A1 and PDE4A8 were found to be significantly up-regulated following USS (summarized in Figure 15). Finally, PDE4D3 was seen to trend towards a significant down-regulation ($p=.089$), while PDE4D9 was seen to trend towards a significant up-regulation following USS ($p=.096$)

Discussion

In summary, we elucidated the BLA whole tissue expression of PDE4 mRNA and confirmed the presence of mature peptide with western blot analysis. Additionally, we narrowed our focus to a specific subpopulation of neurons within the BLA, the principal neuron, and elucidated its expression with scRT-PCR and dual-immunohistochemistry. We found that all of the isoforms we investigated in our study were expressed in BLA whole tissue except for PDE4D1 and PDE4D2. Of those isoforms expressed in BLA whole tissue, PDE4B1, PDE4B2, and PDE4D8 were not expressed in principal neurons. This discrepancy suggests these isoforms are expressed in other cell populations within the BLA. Furthermore, we determined that unpredictable shock stress induces an increase in anxiety-like behavior (Figure 11) and caused region specific alterations in PDE4 isoforms (Figure 12). In particular, PDE4A and PDE4D were altered significantly in whole BLA tissue, whereas PDE4B was altered in BNST, suggesting that different PDE4 isoforms serve differential roles within the emotional circuit.

Baseline PDE4 expression in the BLA

Our study is the first to systematically investigate the baseline expression PDE4 isoforms within the BLA. The driving force behind this study was the clinical trials from the 1980s in which rolipram, a PDE4 inhibitor, was investigated as a potential treatment for depression. In clinical trials, rolipram proved to be highly efficacious and had a rapid onset of action in treating depression; however it also had unwanted emetic side-effects which ultimately prevented its widespread clinical use (reviewed in Zhang, 2009). However, the recognition that the PDE4 family of enzymes may be differentially distributed across the CNS, together with the recent

synthesis of PDE4 isoform-specific pharmacological agents (reviewed in Houslay et al, 2005) has renewed interest in PDE4 inhibitors as potential therapeutic treatments for depression.

Evidence suggests that abnormal activity in the BLA is a key component of the disturbances of emotional circuitry that underlie many affective disorders (Rainnie & Ressler, 2008) and that the PDE4 family of enzymes is a likely candidate underlying both pathology and treatment of affective disorders (Zhang et al., 2002; Zhang et al., 2009; Houslay et al., 2005). Given that little is currently known about the baseline expression of PDE4 isoforms in the BLA, our first priority was to determine which isoforms were present in the BLA under control conditions, and what if any isoforms were expressed by the most abundant cell type in this region, the principal neurons. It is in the BLA principal neurons where fear memories are thought to be formed (reviewed in Maren, 2006; Kim & Jung, 2005) and where aberrant activation is thought to contribute to the development and expression of affective disorders (Rainnie&Ressler, 2008). Hence, identifying PDE4 isoforms that may be selectively expressed in principal neurons of the BLA but not in emetic centers such as the area postrema could help identify novel treatment targets for mood disorders.

Our initial whole tissue PDE4 mRNA analysis revealed that all investigated isoforms of PDE4 were expressed in theBLA, with the exception of PDE4D1 and PDE4D2 (Figure 5). To further evaluate the relative expression of PDE4D1 and PDE4D2 isoforms, we repeated the PCR in triplicate, using the same protocol and the same tissue samples. Occasionally, a faint PCR band would appear at the correct size for either PDE4D1 or PDE4D2, but the expression was inconsistent even within samples suggesting that the PDE4D1 and PDE4D2 isoforms are expressed at levels that are very close to our threshold of detection.

Importantly, our mRNA findings were largely confirmed by our Western blot analysis (Figure 7). Interestingly, our PCR analysis showed an inconsistent, low expression for both PDE4D1 and/or PDE4D2, and a faint, but consistent band was observed at 68kDa, the size of both proteins, in our Western blots. Here, one must recall that levels of mRNA expression, as assayed by RT-PCR, do not necessarily denote the different rates of mRNA turnover (Wilusz, 2001); thus, even low PDE4D1 or PDE4D2 mRNA levels could be translated into consistently detectable amounts of protein. However, this protein band is much fainter than other bands imaged using the same antibody, further supporting the notion that PDE4D1 and PDE4D2 are expressed at very low levels at baseline, just hovering around our threshold of detection. Similarly, the pan-PDE4B antibody failed to label a band where PDE4B3 would be expected to occur, whereas the PDE4B3 isoform specific antibody did (Figure 7), which was consistent with our PCR data showing PDE4B3 transcript expression in the BLA (Figure 5). We performed this blot under identical, controlled conditions several times and yielded consistent results, which suggests that the pan-PDE4B antibody may not be detecting all PDE4B isoforms. Also of note is that, given the predicted band sizes for PDE4A5 (109 Kd), PDE4A8 (106 Kd) and PDE4A10 (108 Kd), it was impossible to determine which of PDE4A5, PDE4A8, and PDE4A10 proteins were expressed. We did have use of a PDE4A5 specific antibody, which did reveal protein expression in the BLA, although this still leaves the protein expression of PDE4A8 and PDE4A10 to be elucidated in future experiments. To better elucidate the baseline protein expression in future studies, we would use isoforms-specific antibodies, as they yielded much clearer and more consistent results across experiments in both Western blot analysis and immunohistochemistry.

Although RT-PCR and Western blot analysis can reveal the presence of different isoforms in whole tissue, they cannot differentiate expression patterns in different neuronal populations within the BLA. scRT-PCR and immunohistochemistry, while not a quantitative method, allowed us to investigate PDE4 expression specifically within the population of principal neurons. Significantly, scRT-PCR revealed that PDE4B1, PDE4B2, and PDE4D8, although expressed in whole tissue, were not expressed in projection neurons at detectable levels. It is unclear at this time whether they are not expressed, or whether they are expressed at levels below our threshold of detection; future protein level analysis will help to elucidate this question. The isoforms expressed in BLA principal neurons via scRT-PCR are also targets for future protein exploration with isoforms-specific antibodies, as the expression of mRNA does not always indicate the presence of mature peptide. It is the mature peptide that catalyzes the breakdown of cAMP, and would thus be the target of pharmacological inhibitors in future drug treatments.

To correlate the mRNA expression profile with the expression of PDE4 protein in BLA principal neurons, we performed a dual-immunofluorescence study for with CaMKII α , a selective marker of principal neurons (Figures 9 & 10). However, while this study was informative, it did not conclusively identify PDE4 isoforms that were selectively expressed by BLA principal neurons. To begin to address this issue we ran a parallel immunofluorescence study to look at selective PDE4 isoform expression in PARV immunoreactive neurons, which make up the second largest population of neurons within the BLA. Our results indicate that the PDE4A5 and PDE4B3 isoforms are both present in principal neurons and in parvalbumin interneurons. However, it should be noted that PDE4 isoforms have differential compartmentalization and differential regulation via ERK and PKA phosphorylation sites

(Zhang, 2009); thus, different isoforms will respond differently to the same treatment. Indeed, a minute difference in expression between these isoforms likely translates into quite varied functional effects on the circuit. Nevertheless, our immunofluorescence study has revealed the basics of how PDE4 may be compartmentalized in the BLA, although we would need to investigate such compartmentalization in the future with antibodies that stain for specific intracellular structures, and using technique such as electron microscopy which can definitively localize the peptides within specific compartments of the cell. With PDE4 isoforms, compartmentalization is the key in keeping the multitude of intracellular signals that interact via the cAMP/PKA cascade separate. This compartmentalization could also prove useful in targeting PDE4 specific inhibitors to the correct subcellular substrate, thereby enhancing the efficacy of the drugs while avoiding unwanted interactions with other PDE4 isoforms.

PDE4 gene expression is altered following unpredictable shock stress (USS)

Once a baseline PDE4 expression in the BLA had been established, we wanted to investigate what happened when the system became stressed. Stress is a common laboratory model for depression (Pollack, 2010), is known to share the same underlying cellular alterations as depression, and is known to precipitate depression and alter the emotional circuitry (Pittenger, 2008; Maroun, 2006; Maroun & Richter-Levin, 2003). Additionally, unpublished observations from our laboratory have demonstrated that principal neurons recorded from BLA slices obtained from USS rats had a reduced threshold for LTP induction; namely, a decrease from a 5x 100 Hz stimulus to a 2x 100 Hz stimulus (Figure 3b). Interestingly, this same reduction in threshold for LTP induction was also observed in control tissue when rolipram was included in the patch solution (Figure 3a). Taken together, this finding suggested that USS may elicit changes in the

cAMP/PKA pathway that mimic PDE4 inhibition. Hence, we predicted that PDE4 expression would be down-regulated in the BLA following USS.

Indeed, we observed a reduction in PDE4A and PDE4D mRNA expression in whole tissue BLA (Figure 12, $p < .05$). Moreover, we observed a six-fold reduction in PDE4D mRNA in single cell mRNA (Figure 14, $p < .001$), accompanied by a reduction in PDE4A that was approaching significance ($p = .056$). The significant decrease in PDE4D is particularly interesting, considering Zhang et al. have proposed that the PDE4D family is the likely candidate involved in depression (Zhang et al, 2002). However, this conclusion is based on the inherent antidepressant-like behavior observed in a line of constitutive PDE4D knockout mice, so the data must be interpreted with caution. Notwithstanding, the difference in PDE4D downregulation between whole tissue and single cell, a 2.5 fold versus 6.2 fold decrease, suggests that principal neurons of the BLA may be unique in their down-regulation of PDE4D. Other neuronal populations present in whole tissue may attenuate this response, perhaps through up-regulation of PDE4D, thus giving the source of the apparent discrepancy and suggesting a role for PDE4D isoforms as the effector subpopulation of PDE4 that is involved in reducing the LTP induction threshold observed in the presence of rolipram.

As reviewed in Rainnie and Ressler, the BLA has a tightly regulated neural circuitry, and disturbances of this circuit likely underlie affective disorders (Rainnie & Ressler, 2008). As such, one would anticipate that PDE4 mRNA may be differentially altered amongst different cell populations. To this end, it would be prudent in a future study to examine PDE4 expression among the interneuron populations of the BLA so that the whole circuit of PDE4 expression may be better elucidated, and analyzed for any potential targets in treating affective disorders.

One limitation of this study was that qPCR probes do not currently exist for the different PDE4 isoforms. To circumvent this problem, we performed densitometric analysis, a semi-quantitative analysis which measures mRNA expression based the intensity of its signal when run in an ethidium bromide gel. The results are summarized in Figure 13 for whole tissue BLA and Figure 15 for single cell principal neurons. Within whole tissue, a robust decrease in signal was detected for multiple PDE4 isoforms. Because densitometric analysis is semi-quantitative, we cannot draw definite conclusions about altered PDE4 gene expression from these results. However, given that the significance level for many of the differences is at the $p < .005$ level, the data does suggest several potential future targets for investigation, specifically PDE4A1, PDE4A8, PDE4B2, PDE4B3, and PDE4D8.

As with baseline expression, we wanted to determine which PDE4 isoforms in principal neurons may be affected by stress. Thus, we performed qualitative PCR comparing PDE4 isoform expression patterns from control and USS rats. There were no obvious gross changes, in that all isoforms present in control tissue were present in USS tissue, and vice versa. Moreover, the number of cells expressing mRNA for different isoforms did not differ significantly between control and USS.

Given the lack of gross changes, we again performed densitometric analysis between the isoforms on single cell cDNA (Figure 15). In contrast to the whole tissue qPCR, whole tissue densitometric analysis, and single cell qPCR (scqPCR), we did not see a robust decrease in PDE4 isoform expression between control and USS. Only two isoforms differed significantly in their expression pattern, PDE4A1 and PDE4A8, and these both showed increased expression, bucking the previous trend. However, PDE4A is significantly downregulated in whole tissue, but not significantly downregulated in single cells; thus, it may also suggest that the bulk of

PDE4A downregulation in whole tissue occurs in interneuron populations. The lack of significant downregulation among isoforms may also be a reflection of the limited sample size available and the sensitivity of the technique; namely, scRT-PCR products must be amplified before screening so that there is sufficient cDNA for detection. Moreover, densitometry is only a semi-quantitative method of analysis, and may not be sensitive enough to detect changes at the single cell level. Thus, the lack of significant results may reflect sensitivity limitations of the technique that could be corrected with the use of quantitative probes in a future experiment.

Future Directions

Although we have begun to elucidate PDE4 expression in the BLA, our findings are far from complete. Given that mRNA expression does not always equate to presence of the mature peptide, it would be prudent to perform Western Blot analysis and dual-immunofluorescence studies on BLA samples with a wider spectrum of commercially available PDE4 isoform-specific antibodies. However, financial constraints restricted our analysis to those that we considered as likely candidates to change. Furthermore, our densitometric analysis is only semi-quantitative, and although it did suggest several targets for change, we cannot ascertain for sure whether mRNA expression is altered based on these findings alone. However, densitometric analysis has suggested several target PDE4 isoforms to investigate with qPCR, Western Blot analysis, and co-immunohistochemistry in the future.

Additionally, this experiment has focused mainly on principal neurons within the BLA. Although these represent 80% of the total neuronal population, BLA interneurons are important in maintaining the basal level of activity in the circuit. As such, these populations of interneurons are also likely to be subject to stress-induced PDE4 alterations; investigation of interneuronal

populations using these same techniques in the future will give us a better notion of the gross altered activity of the BLA.

Finally, we must remember that the BLA is only one part of the complex emotional circuitry involved in affect and affective disorders. Indeed, given the fMRI evidence that the BLA is hyperactive in depressed patients (Drevets, 2003), and that the BLA appears hyperactive *in vitro* following stress (Li and Rainnie, unpublished observations, Figure 3b), it seems contradictory that rolipram, which also causes hyperactivity of BLA principal neurons *in vitro* (Li and Rainnie, unpublished observations, Figure 3a), would be a viable treatment for affective disorders. However, rolipram was quite effective and had a much faster onset of efficacy than other pharmacological agents available, with patients demonstrating a significant decrease in their HAM-D score by day 14 of the study (Fleishhacker, 1992); its use as an antidepressant was only precluded by emetic side effects (Zhang, 2009). To this end, it seems clear that other brain regions involved in depression, such as the medial prefrontal cortex (mPFC), the subgenual cingulate cortex (SCC), and the hippocampus, which are known components of the emotional circuitry (Pittenger, 2008; Drevets, 2003), must also be evaluated for baseline PDE4 expression before an isoforms-specific inhibitor can be considered as a potential antidepressant treatment. Also, given the history of emetic side effects, it would be prudent to investigate PDE4 expression in the area postrema, the emetic center of the brain as well, to prevent such side effects from occurring in the future.

Although much work remains before PDE4 inhibitors can be truly evaluated as pharmacological treatments for depression, we have taken an important first step in determining baseline PDE4 expression in the BLA, an affective locus in the brain, and determining what happens to that locus when it comes under stress.

Figures

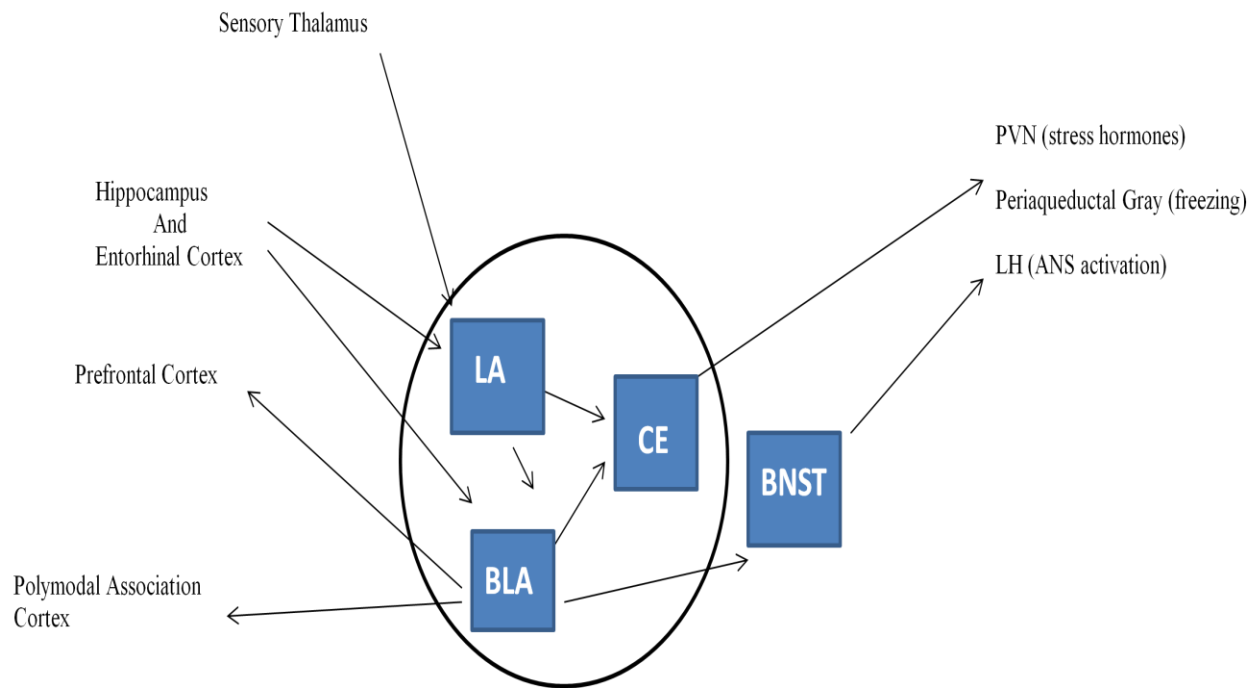


Figure 1: A simplified representation of the inputs and outputs of the BLC, adapted from *LeDoux, 2007*.

Inputs enter the amygdala at the LA and BLA, then project out through the CE and the BNST.

Abbreviations: LA, Lateral nucleus of the amygdala; CE, central nucleus of the amygdala; BLA, basolateral nucleus of the amygdala; PVN, paraventricular nucleus of the hypothalamus; LH, lateral hypothalamus.

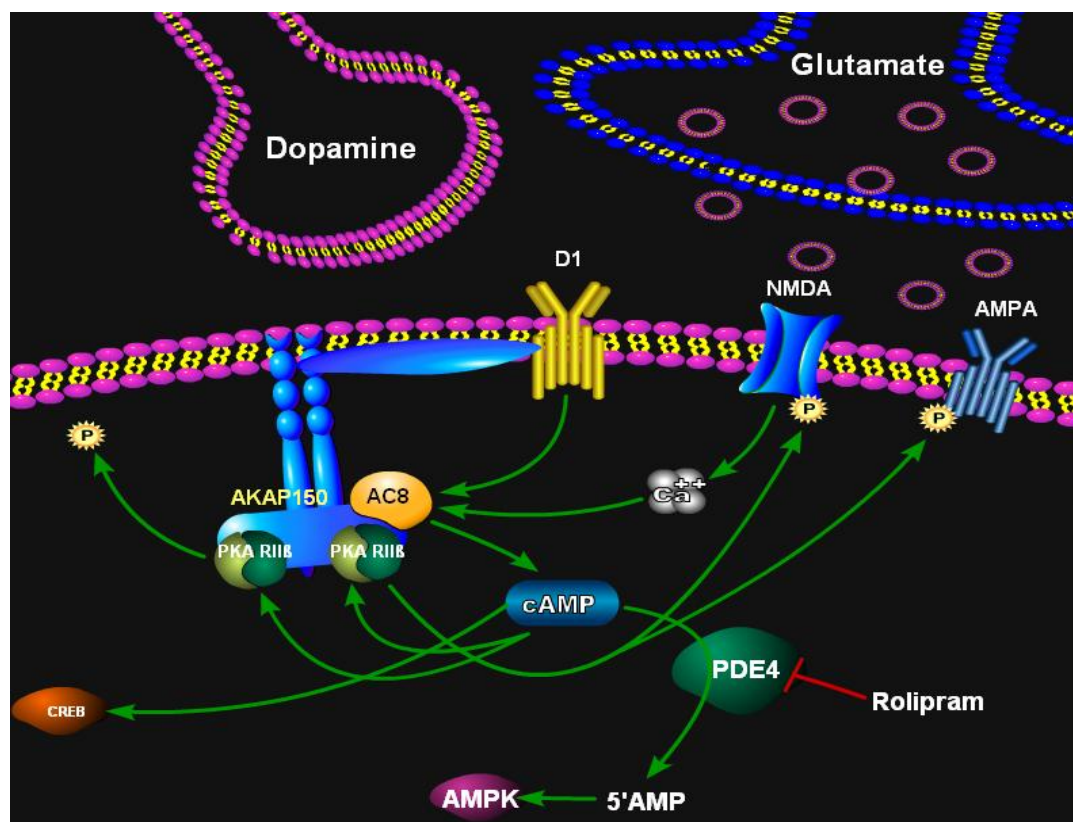


Figure 2: A schematic summarizing the cAMP/PKA cascade in the BLA related to dopaminergic transmission.

Dopamine activates D1 receptors, causing the G_{αs} subunit to disassociate and activate adenylylacyclase (AC). AC catalyzes the conversion of ATP into cAMP, which then activates protein kinase A (PKA). PKA activates a plethora of downstream targets, including the cAMP response element binding protein, a transcription factor. cAMP levels are returned to baseline via the phosphodiesterases, including PDE4. PDE4 is inhibited by rolipram.

Image courtesy of Dr. Donald Rainnie, Ph.D.

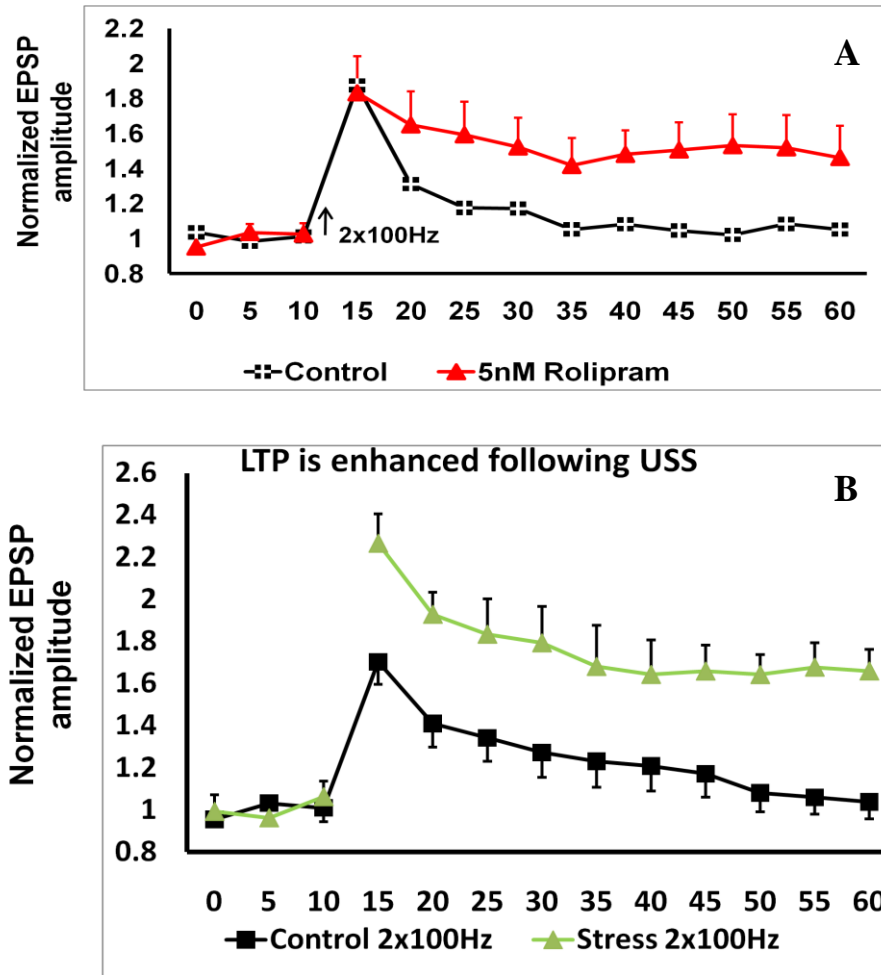


Figure 3: Administration of rolipram mimics the USS decrease in LTP induction threshold.

A) Administration of rolipram, a PDE4 inhibitor, reduced the threshold for LTP induction in the BLA. In control conditions, a 5x 100Hz stimulus is required for LTP induction. Following administration of rolipram, this is reduced to 2x 100 Hz stimulus.

B) Following USS, the threshold for LTP induction is reduced to a 2x 100 Hz stimulus from the baseline 5x 100 Hz stimulus. Here, we see that the threshold for LTP induction is not altered in littermate controls who were exposed to the shock apparatus for an equivalent amount of time but did not receive shock.

Data are courtesy of Dr. Chen-Chen Li, Ph.D.

PDE4 isoform	Forward	Reverse	PCR product size (bp)
PDE4A1	TTCTTCTGCGAGACCTGCTCCAAGC	CAGGCCCCATTGCTCAAGTTCTCC	372
PDE4A5	AAGGAGCCTGTCTCTCTCTTCCG	GGTACCGGTGCCGTGGAAGGA	259
PDE4A8	GCCCAGAGAGGCTTGGTGATTTATCC	ATATTCGAGGCAGTGTGAGCCTTTGC	215
PDE4A10	GCATTGCCCTAGGACCAGAGTC	CAAGCTGACACATCTGCCCGGAG	90
PDE4B1	AAACCTTACGGAGCACCGAACAAAGAGG	GCCACGTTGAAGATGTTAAGGCCCCATT	506
PDE4B2	TTGGTAGATCACTGACACCTCATCCCG	GCCACGTTGAAGATGTTAAGGCCCCATT	667
PDE4B3	CTCCACGCAGTTCACCAAGGAAC	TGTGTGAGCTCCCGGTTGAGC	598
PDE4B4	ATGGGGGCCGTCATGGGCAC	ACCACACCACTGGGGCACTCG	252
PDE4D1	ACGTCAAGCTGGAGCATCTCGGC	GATCCTACAACATGTATTGCACTGGC	928
PDE4D2	ACGTCAAGCTGGAGCATCTCGGC	GATCCTACAACATGTATTGCACTGGC	842
PDE4D3	CTAATTTTGCAAGATCGCGACCCAGC	GCTGGTTTGCCAGACCGACTCATTCA	254
PDE4D4	AGCGCTACCTGTACTGTCTG	GACTCCACTTGATCTGAGACATTG	764
PDE4D5	TGCCAGCTGTACAAAGTTGACc	TTCTCGGAGAGATCACTGGAGA	212
PDE4D7	GAGCACTGACTTTGGAAGCAGCTAGTGTGGCATC	GTCAGAGGCCGGTTGCCAGACAGCTCC	400
PDE4D8	GCTCTGACTTCTCGTGGTTCCTGGGGATCTGG	GACCGACTCATTTCAGAGAGATGGGTGAGCTCC	120
PDE4D9	CTCCAAACCTTCTTTGTGGAGAG	TTACGTATCAGGACACAGCAGTG	301

Table 1: PCR primer pairs and final products sizes

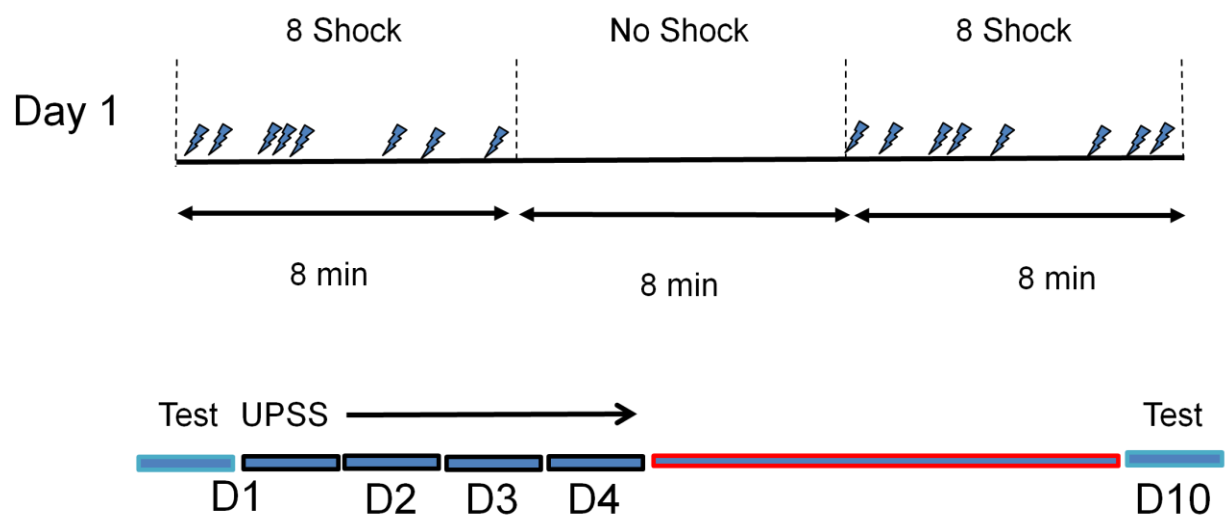


Figure 4: An illustration of the Unpredictable Shock Stress (USS) paradigm.

Rats are pretested for startle behavior before day 1 and distributed across groups such that the mean baseline startle is the same for both the control group and the experimental group.

Following a five minute attenuation period, rats receive two treatments of eight (8) randomized shocks over eight (8) minutes, separated by an eight (8) minute rest period. Rodents receive shock for four consecutive days and are sacrifice on day ten (10) of the experiment.

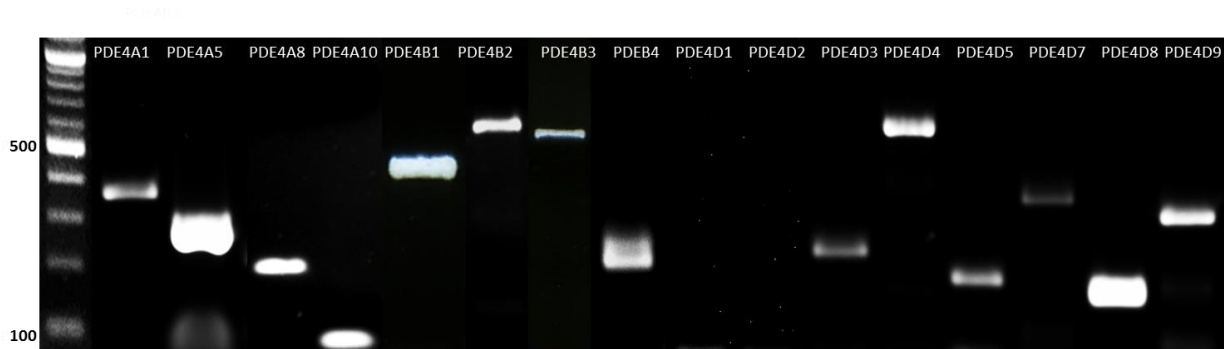


Figure 5: RT-PCR reveals the expression of PDE4 splice variants in the BLA

RT-PCR analysis revealed the expression of all PDE4 splice variants investigated, with the exception of PDE4D1 and PDE4D2 (MW 928 and 842, respectively).

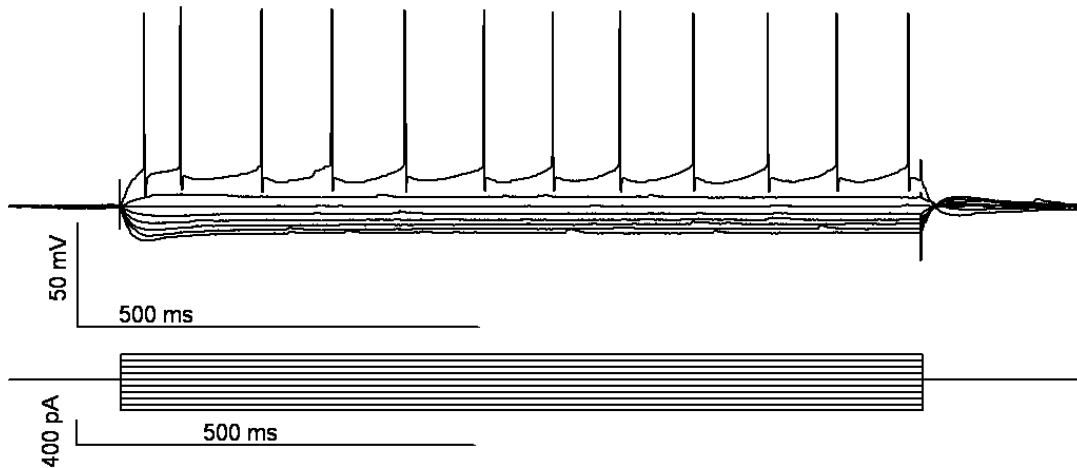
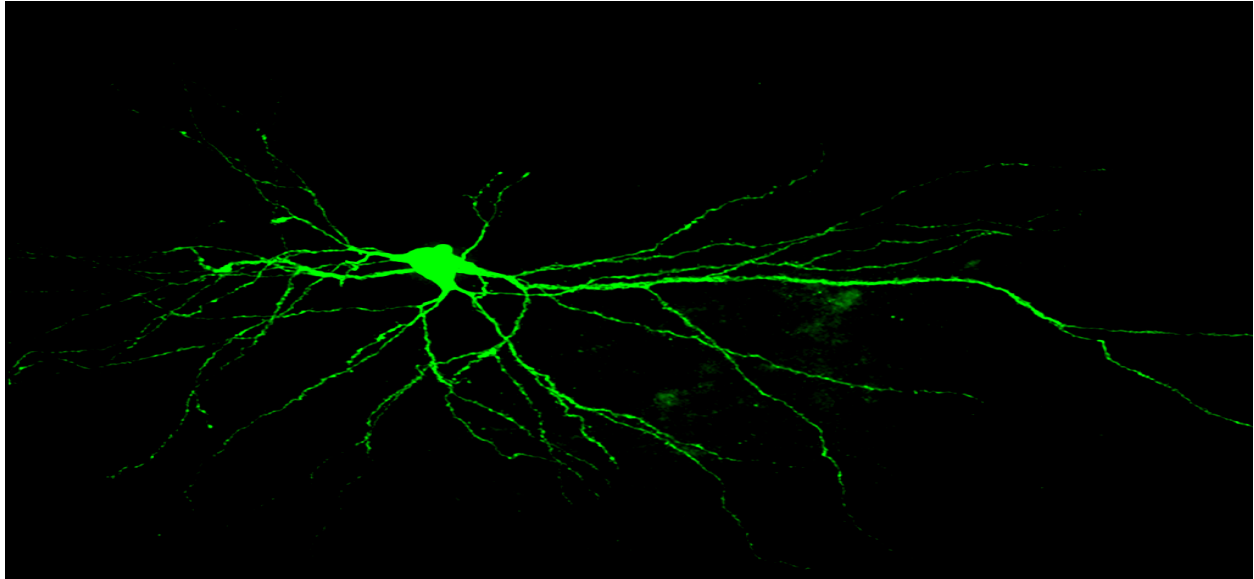


Figure 6: *BLA principal neurons have stereotyped anatomy and electrophysiological properties.*

Here is an example of a principal BLA neuron along with a sample of its electrophysiological profile. Principal neurons can be identified based on their physiological properties, including input resistance, spike train properties, and expression of voltage-dependent currents such as I_h and I_t . Here, the neuron was filled with biocytin and stained with streptavidin, then processed for immunohistochemistry.

Image is courtesy of Steven J. Ryan, B.S., Ph.D candidate

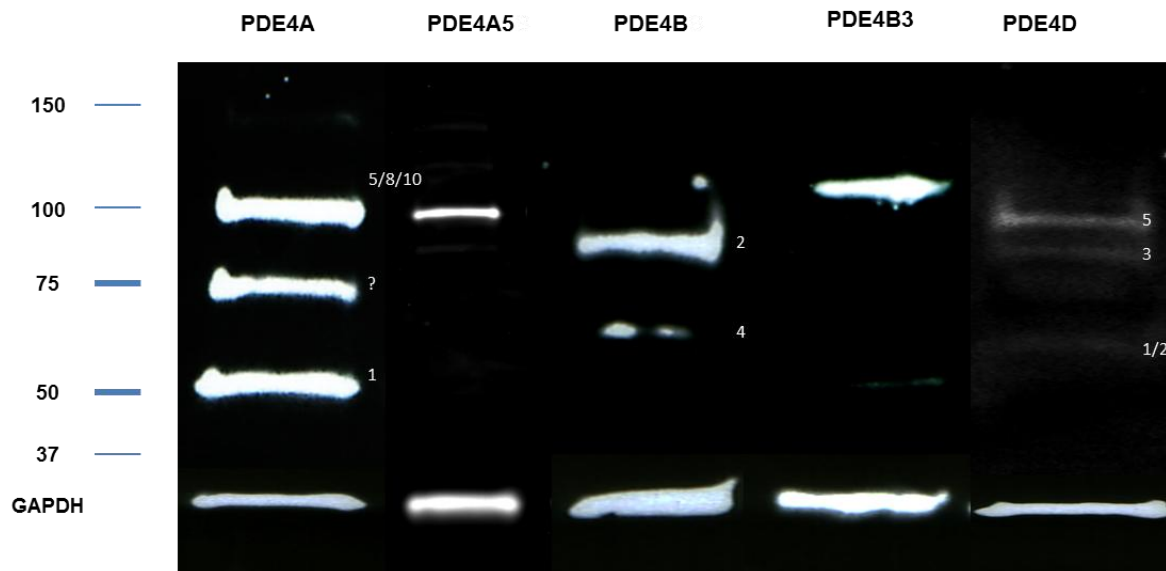


Figure 7: Western Blot analysis confirms the presence of mature PDE4 peptide isoforms in the BLA.

To confirm the presence of mature peptide, western blot assay was used to examine protein expression in the BLA. Multiple bands were observed for each of the pan PDE4 antibodies, all of which correspond to whole tissue mRNA expression. Interestingly, we detected a faint band at the correct size for PDE4D1 and PDE4D2 (68 kDa, indistinguishable based on size). Much like mRNA expression, this band was very faint, suggesting that PDE4D1 and/or PDE4D2 are expressed at very low levels in the BLA, bordering just at our threshold of detection.

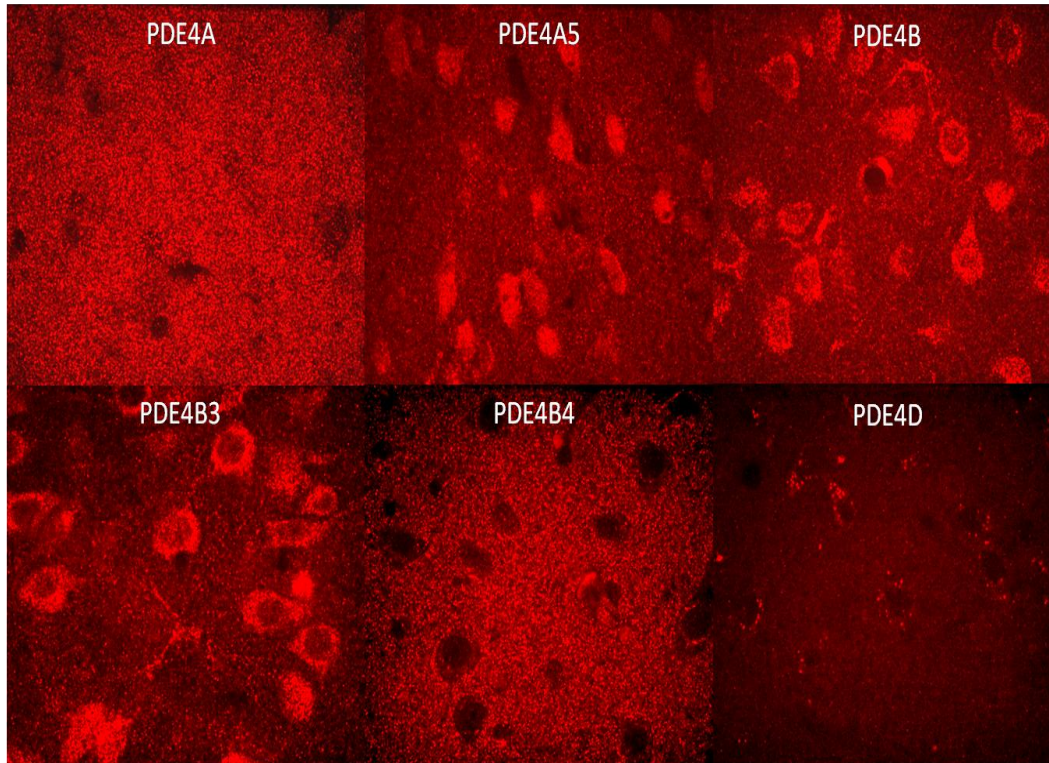


Figure 8: *Immunohistochemical investigation reveals that PDE4 isoforms are differentially expressed within BLA cell populations.*

Immunohistochemistry reveals the presence of PDE4A pan, PDE4A5, PDE4B pan, PDE4B3, PDE4B4, and PDE4D panenzyme in whole BLA slices. PDE4A appears richly expressed throughout the sample, whereas PDE4A5 is localized mostly to the soma, suggesting that other PDE4 isoforms are more richly expressed in the neuropil. In contrast, PDE4B pan appears mainly localized to the soma, although it is expressed in neuropil. PDE4B3 is highly expressed in the soma, whereas PDE4B4 seems relegated to the neuropil. In contrast to both schemes above, pan PDE4D seems to be localized at an unidentified intracellular structure.

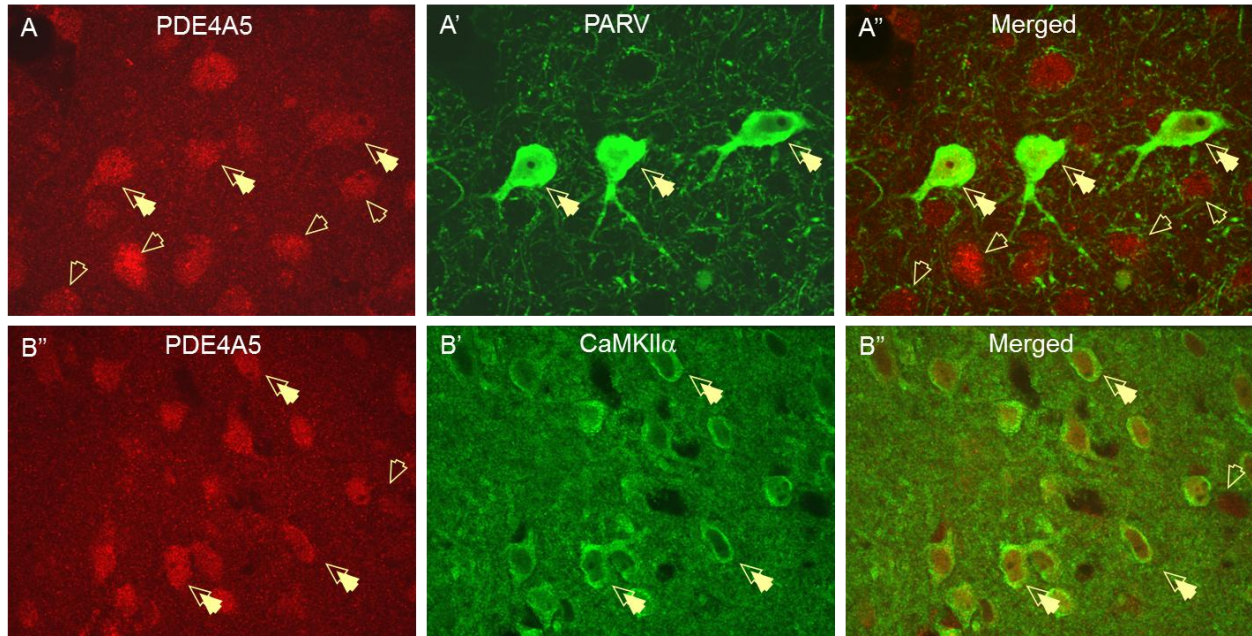


Figure 9: Dual Immunohistochemistry reveals the presence of PDE4A5 in both parvalbumin-immunoreactive(PARV) interneurons and glutamatergic principal BLA neurons

A-A'' At 63x magnification, we see co-labeling for PDE4A5 (**A**, red, opened arrows) and PARV (**A'**, green, closed arrows) in the BLA (**A''**, merged) represented by the double arrows. Open arrows demonstrate labeling of PDE4A5 alone. All PARV interneurons in the sample appeared to co-express PDE4A5, but not all PDE4A5 positive neurons are PARV, suggesting the presence in another cell population.

B-B'' At 63x magnification, we see co-labeling for PDE4A5 (**B**, red, opened arrows) and CaMKII α (**B'**, green, closed arrows), a marker of projection neurons in the BLA (**B''**, merged). We see that all principal neurons express PDE4A5, but that some PDE4A5 staining does not co-localize with CamKII α , suggesting expression in an interneuronal population.

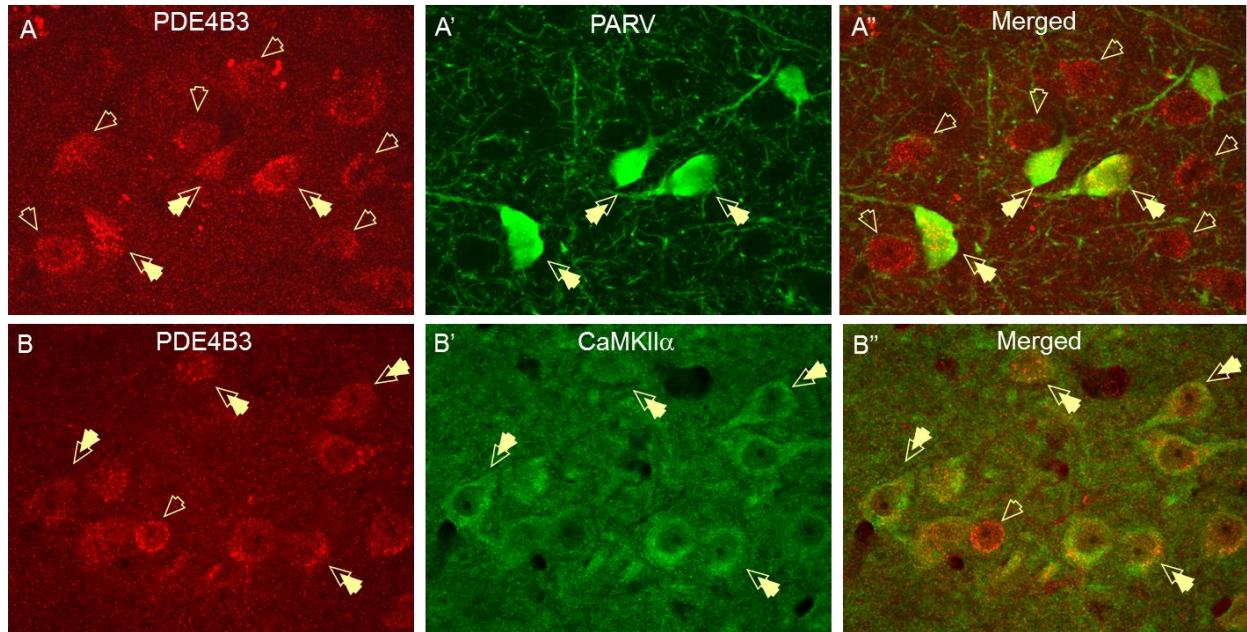


Figure 10: Dual immunohistochemistry reveals the expression of PDE4B3 in both parvalbumin-positive (PARV) interneurons and glutamatergic principal neuron populations.

A-A'' At 63x magnification, we see that PDE4B3 (A, red, opened arrow) co-localizes with PARV (A', green, closed arrow) in the BLA (A'', merged). However, we see that PDE4B3 is robustly expressed outside of PARV interneurons, suggesting its expression is not unique to this cell population

B-B'' Here, we see that PDE4B3 (B, red, opened arrow) and CaMKIIα (B', green, closed arrow) are expressed in whole tissue BLA (B'', merged). Again, we also see PDE4B3 not co-localized with CamKIIα, demonstrating that PDE4B3 is not unique to one neuronal population in the BLA.

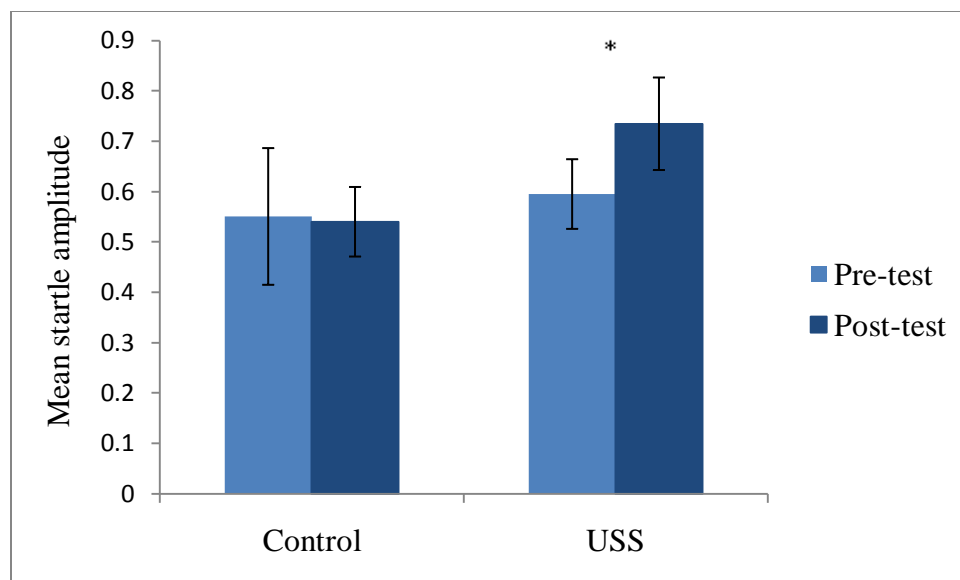


Figure 11: A histogram showing that USS facilitates the acoustic startle response

Here, we see that following USS, rats expressed enhanced average acoustic startle to 100, 105, and 110 db tones ($p < .05$) that is not observed in control littermates (student's paired t-test).

There is no significant difference in initial startle between the control and USS group ($p = 0.77$, student's unpaired t-test), demonstrating that this change is due to the treatment between the groups and not any initial differences within the groups.

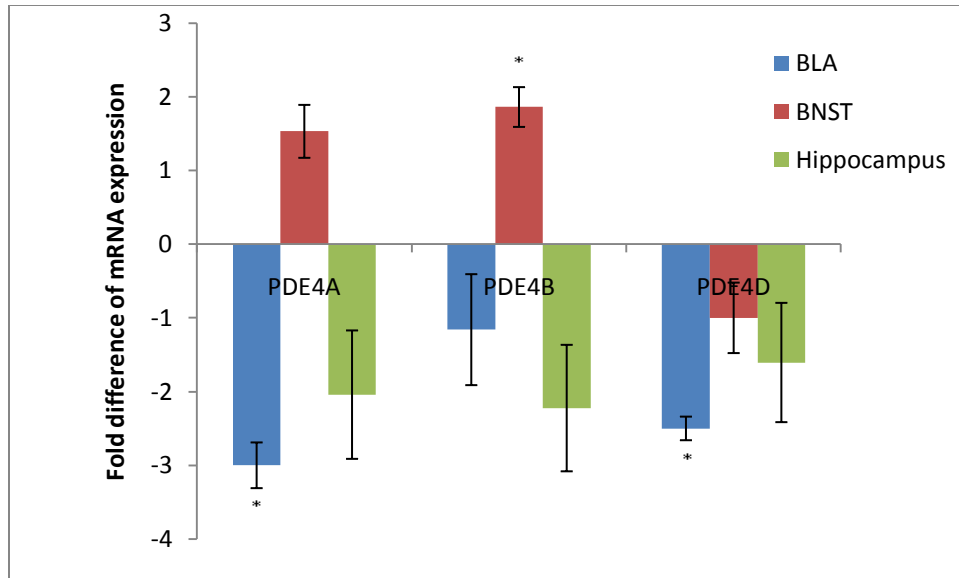


Figure 12: Whole Tissue qPCR reveals that pan PDE4 mRNA is differentially altered following USS.

qPCR analysis reveals that PDE4A and PDE4D are significantly downregulated in the BLA and PDE4B is significantly upregulated in the BNST following USS ($p < .05$). Furthermore, PDE4 was not significantly altered in the hippocampus following USS. Here, we see that one alteration, USS, has differential effects on differential PDE4 families within the emotional circuitry.

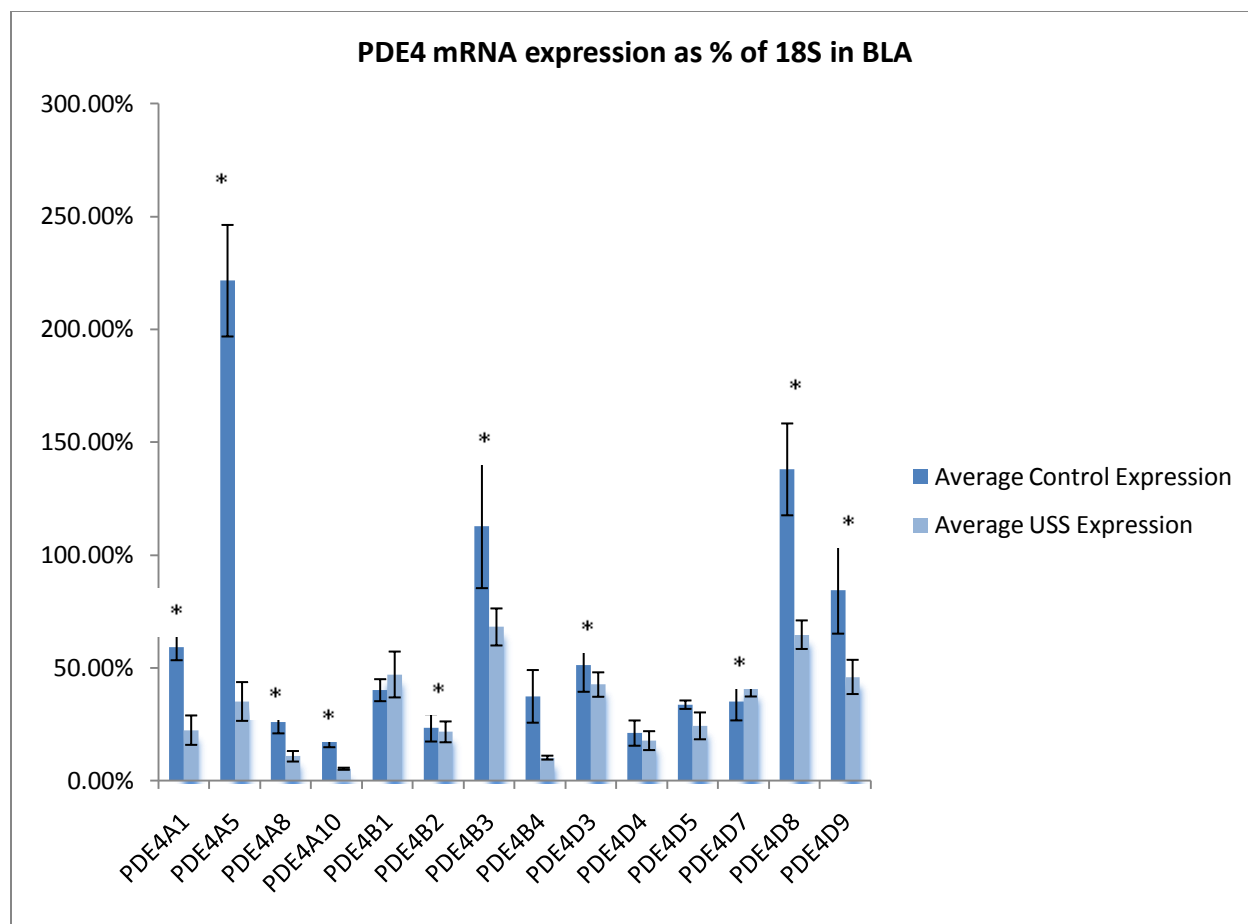


Figure 13: A histogram showing the relative change in expression of PDE4 isoform mRNA in the BLA from control and USS rats as determined by whole tissue densitometric analysis.

Whole tissue densitometric analysis, while not quantitative, reveals several PDE4 isoforms that appear to be significantly down-regulated following USS (asterisks = $p < .05$). These PDE4 isoforms suggest follow up analysis using qPCR in a future study.

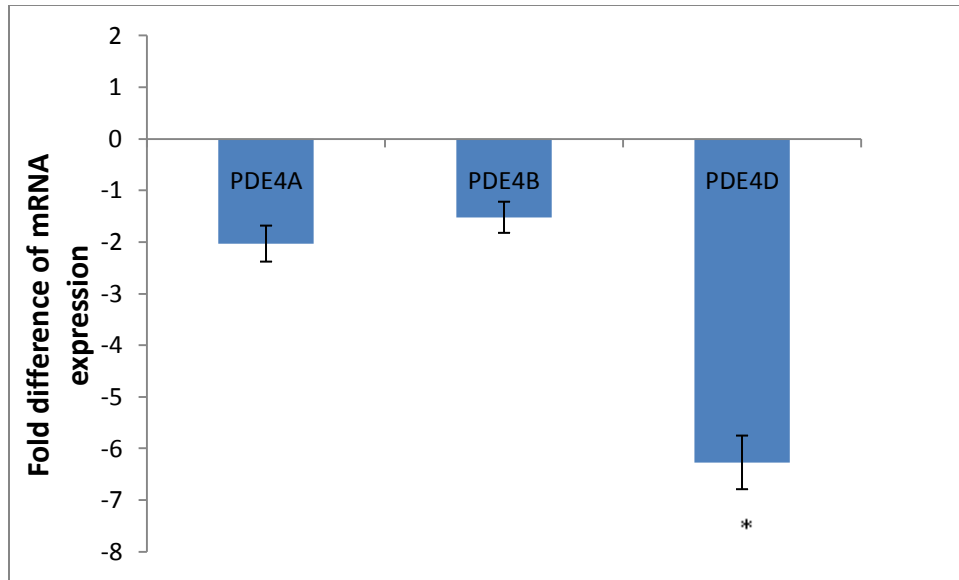


Figure 14: A histogram showing the effects of USS on pan PDE4 isoform expression in BLA principal neurons as determined by single cell qPCR.

Single Cell qPCR reveals a 6.2 decrease in the fold expression of PDE4D following USS ($p < .05$) and a decrease in PDE4A that is approaching significance ($p = .056$), mimicking the results found in whole tissue.

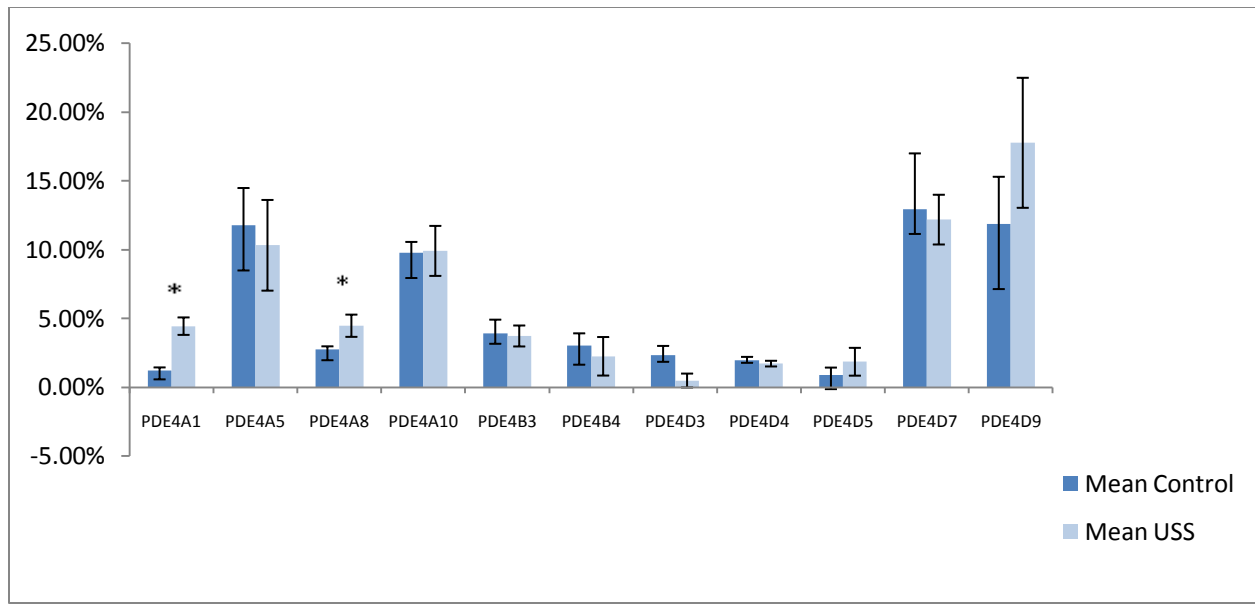


Figure 15: A histogram showing the effects of USS on PDE4 isoform expression in BLA principal neurons as determined by single cell densitometric analysis.

Single cell densitometric analysis did not reveal robust differences in PDE4 gene expression following USS as compared to controls, except in the case of PDE4A1 and PDE4A8 ($p < .05$).

References

- Andrade, C., & Rao, N. S. K. (2010). How antidepressant drugs act: A primer on neuroplasticity as the eventual mediator of antidepressant efficacy. *Indian journal of psychiatry*, 52(4), 378-386.
- Bolger, G. B., Rodgers, L., & Riggs, M. (1994). Differential CNS expression of alternative mRNA isoforms of the mammalian genes encoding cAMP-specific phosphodiesterases. *Gene*, 149(2), 237-44.
- Dabrowska, J and Rainnie, D.G. (2010). Expression and distribution of Kv4 potassium channel subunits and potassium channel interacting proteins in subpopulations of interneurons in the basolateral amygdala. *Neuroscience*. 171(3), 721-733.
- Davis M, Walker DL, Lee Y.(1997). Amygdala and bed nucleus of the striaterminalis: differential roles in fear and anxiety measured with the acoustic startle reflex. *Philosophical transactions of the Royal Society of London. Series B, Biological sciences*. 352(1362):1675-87.
- Davis, M., Rainnie, D., & Cassell, Martin.(1994). Neurotransmission in the rat amygdala related to fear and anxiety. *Trends in Neuroscience*. 17(5), 208-14.
- Drevets, W. C. (1999). Prefrontal cortical-amygdalar metabolism in major depression. *Annals of the New York Academy of Sciences*, 877, 614-37.
- Fadok, J.P., Dickerson, T.M.K., & Palmiter, R.D. (2009). Dopamine is Necessary for Cue-Dependent Fear Conditioning. *The Journal of Neuroscience*. 29(36). 11089-11097.
- Fleischhacker, W., Hinterhuber, H., Bauer, H., Pflug, B., Berner, P., Simhandl, C., Wolf, R., Gerlach, W., Jaklitsch, H., Sastre-y-Hernandez, M., Schmeding-Wiegel, H., Sperner-Unterweger, B., Voet, B., Schubert, H. (1992). A multicenter double-blind study of three

different doses of the new cAMP-phosphodiesterase inhibitor rolipram in patients with major depressive disorder. *Neuropsychobiology*, 26(1-2), 59–64. Karger Publishers.

- Fox, J.H., Hammack, S.E., & Falls, W.A. (2008). Exercise is associated with reduction in the anxiogenic effect of mCPP on acoustic startle. *Behavioral Neuroscience*. 122(4).943-8.
- Guo, J.D. & Rainnie, D.G. (2010) Presynaptic 5-HT_{1B} receptors-mediated serotonergic inhibition of glutamate transmission in the bed nucleus of the stria terminalis. *Neuroscience*, 165(4), 1390–1401.
- Hazra, R., Guo, J.D., Ryan, S.J., Jasnow, A.M., Dabrowska, J., & Rainnie, D.G. (2011). A transcriptomic analysis of type I-III neurons in the bed nucleus of the stria terminalis. *Molecular and Cellular Neuroscience*, 46(4), 699-709.
- Herbert, J., Goodyer, I. M., Grossman, a B., Hastings, M. H., Kloet, E. R. de, Lightman, S. L., et al. (2006). Do corticosteroids damage the brain?. *Journal of Neuroendocrinology*, 18(6), 393-411.
- Houslay, M. D., Baillie, G. S., & Maurice, D. H. (2007). cAMP-Specific phosphodiesterase-4 enzymes in the cardiovascular system: a molecular toolbox for generating compartmentalized cAMP signaling. *Circulation research*, 100(7), 950-66.
- Houslay, M.D., Schafer, P., & Zhang, K.Y.J. (2005). Keynote Review: Phosphodiesterase-4 as a therapeutic target. *Drug Discovery Today*, 10(22), 1503-19.
- Huang, Y. & Kandel, E. (1998). Post-synaptic induction and PKA-Dependent Expression of LTP in the Lateral Amygdala. *Neuron*. 21(1). 169-78
- Hubbard, D.T., Nakashima, B.R., Lee, I., & Takahashi, L.K. (2007). Activation of Basolateral Amygdala Corticotropin-Releasing Factor 1 Receptors Modulates the Consolidation of Contextual Fear. *Neuroscience*. 150(4).818-28.

- Itoh, T. (2003). Different regulation of adenylyl cyclase and rolipram-sensitive phosphodiesterase activity on the frontal cortex and hippocampus in learned helplessness rats. *Brain Research*, 991(1-2), 142-149.
- Jessel, T.M. & Sanes, J.R.. (2000). The Generation and Survival of Neural Cells. In E.R. Kandel, J.H. Schwartz, & T.M. Jessel (Eds.), *Principles of Neural Science, 4th Edition*. (pp.1041-62). New York: McGraw Hill.
- Kandel, E.R. (2000). Cellular Mechanisms of Learning and the Biological Basis of Individuality. In E.R. Kandel, J.H. Schwartz, & T.M. Jessel (Eds.), *Principles of Neural Science, 4th Edition*. (pp.1247-79). New York: McGraw Hill.
- Kim, J.J. & Jung, M.W. (2006). Neural circuits and mechanisms involved in pavlovian fear conditioning: A critical review. *Neuroscience and Biobehavioral Reviews*, 30(1), 188-202.
- LeDoux, J. E. (2003). The emotional brain, fear, and the amygdala. *Cellular and molecular neurobiology*, 23(4-5), 727-38.
- LeDoux, J. E. (2007). The amygdala. *Current Biology*, 17(20), R868-74.
- Lodish, H., Berk, A., Kaiser, C.A., Krieger, M., Scott, M.P., Bretscher, A., Ploegh, H., & Matsudaira, P. (Eds). (2008). Cell Signaling I: Signal Transduction and Short-Term Cellular Responses. *Molecular Cell Biology, 6th Edition*. (pp.623-64) New York: W.H. Freeman and Company
- Maren, S. (2006). The amygdala, synaptic plasticity, and fear memory. *Annals of the New York Academy of Sciences*, 985(1), 106-13
- Maroun, M. (2006). Stress reverses plasticity in the pathway projecting from the ventromedial prefrontal cortex to the basolateral amygdala. *The European journal of Neuroscience*, 24(10), 2917-22.

- Maroun, M., & Richter-Levin, G. (2003). Exposure to acute stress blocks the induction of long-term potentiation of the amygdala-prefrontal cortex pathway in vivo. *The Journal of Neuroscience: the official journal of the Society for Neuroscience*, 23(11), 4406-9.
- McDonald, A.J. (1998). Cortical Pathways to the mammalian amygdala. *Progress in Neurobiology*, 55(3), 257-332.
- McPhee, I., Cochran, S., & Houslay, M. D. (2001). The novel long PDE4A10 cyclic AMP phosphodiesterase shows a pattern of expression within brain that is distinct from the long PDE4A5 and short PDE4A1 isoforms. *Cellular Signaling*, 13(12), 911-8.
- Miro, X., Perez-Torres, S., Puigdomenech P., Palacios J.M., & Mengod, G. (2002). Differential distribution of PDE4D splice variant mRNAs in rat brain suggests association with specific pathways and presynaptic localization. *Synapse*, 45(4), 259-69
- Muly, E.C., Senyuz, M., Khan, Z.U., Guo, J.D., Hazra, R. & Rainnie, D.G. (2009). Distribution of D1 and D5 dopamine receptors in the primate and rat basolateral amygdala. *Brain Structure & Function*. 213(4-5), 375-93
- O'Donnell, J.M. & Zhang, H.T. (2004). Antidepressant effects of inhibitors of cAMP phosphodiesterase (PDE4). *Trends in Pharmacological Science*, 25(3), 158-63.
- Pitkänen, A., Savander, V, and LeDoux, J. (1997) Organization of intra-amygdaloid circuitries in the rat: an emerging framework for understanding functions of the amygdala. *Trends in Neuroscience*. 20 (11), 517-523
- Perez-Torres, Miro, X., Palacios, J.M., Cortes, R., Puigdomenech P., & Mengod, G. 2000). Phosphodiesterase Type 4 isozymes expression in human brain examined by in situ hybridization histochemistry and [3H]rolipram binding autoradiography. Comparison with monkey and rat brain. *Journal of Chemical Neuroanatomy*, 20(3-4), 349-74

- Pittenger, C., & Duman, R. S. (2008). Stress, depression, and neuroplasticity: a convergence of mechanisms. *Neuropsychopharmacology : official publication of the American College of Neuropsychopharmacology*, 33(1), 88-109.
- Pollak, D. D., Rey, C. E., & Monje, F. J. (2010). Rodent models in depression research: classical strategies and new directions. *Annals of medicine*, 42(4), 252-64.
- Rainnie, D.G. & Ressler, K.J. (2009). Physiology of the Amygdala: Implications for PTSD. In Priyattam J. Shiromani & Terence M. Keane & Joseph E LeDoux (Eds.), *Post-Traumatic Stress Disorder: Basic Science and Clinical Practice* (39-78). New York, NY: Humana Press
- Rattiner, L. M., Davis, M., & Ressler, K. J. (2005). Brain-derived neurotrophic factor in amygdala-dependent learning. *The Neuroscientist*, 11(4), 323. SAGE Publications.
- Rau, V., DeCola, J.P., & Fanselow, M.S. (2005). Stress-induced enhancement of fear learning: an animal model of post-traumatic stress disorder. *Neuroscience and Biobehavioral Reviews*. 29(8). 1207-23.
- Ressler, K. J., & Nemeroff, C. B. (2000). Role of serotonergic and noradrenergic systems in the pathophysiology of depression and anxiety disorders. *Depression and Anxiety*, 12(S1), 2-19. Wiley Online Library.
- Siegelbaum, S.A, Schwartz, J.H., & Kandel, E.R. (2000). Modulation of Synaptic Transmission: Second Messengers. In E.R. Kandel, J.H. Schwartz, & T.M. Jessel (Eds.), *Principles of Neural Science, 4th Edition*. (pp.229-51). New York: McGraw Hill.
- Takahashi, M., Terwilliger, R., Lane, C., Mezes, P. S., Conti, M., Duman, R. S., et al. (1999). Chronic antidepressant administration increases the expression of cAMP-specific phosphodiesterase 4A and 4B isoforms. *The Journal of neuroscience : the official journal of the Society for Neuroscience*, 19(2), 610-8.

- Walker, D. (2003). Role of the bed nucleus of the striaterminalis versus the amygdala in fear, stress, and anxiety. *European Journal of Pharmacology*, 463(1-3), 199-216.
- Wilusz, C. J., Wormington, M., & Peltz, S. W. (2001). The cap-to-tail guide to mRNA turnover. *Nature reviews. Molecular cell biology*, 2(4), 237-46.
- Ye, Y., Jackson, K., & O'Donnell, J. M. (2000). Effects of repeated antidepressant treatment of type 4A phosphodiesterase (PDE4A) in rat brain. *Journal of neurochemistry*, 74(3), 1257-62.
- Zhang, H.T. (2009). Cyclic AMP-specific phosphodiesterase-4 as a target for the development of antidepressant drugs. *Current pharmaceutical design*, 15(14), 1688-98.
- Zhang, H.T., Huang, Y., Jin, S.L.C., Frith, S.A., Suvarna, N., Conti, M., & O'Connell, J.M. (2002). Antidepressant-like profile and reduced sensitivity to rolipram in mice deficient in the PDE4D phosphodiesterase enzyme. *Neuropsychopharmacology : official publication of the American College of Neuropsychopharmacology*, 27(4), 587-95.